

Alma Mater Studiorum Università di Bologna
Archivio istituzionale della ricerca

Immunolocalization of Vasa, PIWI, and TDRKH proteins in male germ cells during spermatogenesis of the teleost fish *Poecilia reticulata*

This is the final peer-reviewed author's accepted manuscript (postprint) of the following publication:

Published Version:

Milani L., Cinelli F., Iannello M., Lazzari M., Franceschini V., Maurizii M.G. (2022). Immunolocalization of Vasa, PIWI, and TDRKH proteins in male germ cells during spermatogenesis of the teleost fish *Poecilia reticulata*. ACTA HISTOCHEMICA, 124(3), 1-12 [10.1016/j.acthis.2022.151870].

Availability:

This version is available at: <https://hdl.handle.net/11585/890211> since: 2024-05-21

Published:

DOI: <http://doi.org/10.1016/j.acthis.2022.151870>

Terms of use:

Some rights reserved. The terms and conditions for the reuse of this version of the manuscript are specified in the publishing policy. For all terms of use and more information see the publisher's website.

This item was downloaded from IRIS Università di Bologna (<https://cris.unibo.it/>).
When citing, please refer to the published version.

(Article begins on next page)

This is the peer reviewed version of the following article:

L. Milani, F. Cinelli, M. Iannello, M. Lazzari, V. Franceschini, M.G. Maurizii. Immunolocalization of Vasa, PIWI, and TDRKH proteins in male germ cells during spermatogenesis of the teleost fish *Poecilia reticulata*. Acta Histochemica. 2022;124:151870.

which has been published in final form at

<https://doi.org/10.1016/j.acthis.2022.151870>.

This article may be used for non-commercial purposes in accordance with Elsevier Terms and Conditions for Use of Self-Archived Versions.

Immunolocalization of Vasa, PIWI, and TDRKH proteins in male germ cells during spermatogenesis of the teleost fish *Poecilia reticulata*

L. Milani, F. Cinelli, M. Iannello, M. Lazzari, V. Franceschini, M.G. Maurizii
Department of Biological, Geological, and Environmental Sciences, University of Bologna,
Bologna, Italy

Corresponding authors at: Department of Biological, Geological, and Environmental Sciences,
University of Bologna, Via Selmi 3, 40126, Bologna, Italy.

E-mail address: liliana.milani@unibo.it (L. Milani); maria.maurizii@unibo.it (M.G. Maurizii).

Abstract

Vasa, PIWI and TDRKH are conserved components of germ granules that in metazoans are involved in germline specification and differentiation, as documented by mutational experiments in some model animals. So far, investigations on PIWI during spermatogenesis of fish has been limited to a few species, and no information is available for TDRKH, another protein involved in the piRNA pathway. In this study, the immunolocalization of these three germline determinants was analyzed in male gonads of the teleost fish *Poecilia reticulata* to document their localization pattern in the different stages of germ cell differentiation.

To analyze their distribution pattern during the different stages of spermatogenesis we performed immunohistochemistry (IHC) and immunofluorescence (IF) assays using primary polyclonal antibodies after testing their specificity with Western Blot. Moreover, sections of testis stained with haematoxylin and eosin clarified the structural organization of *P. reticulata* testis, while the use of the confocal microscope and the nuclear staining clarified the different stages of germ cell differentiation during spermatogenesis.

The results showed that Vasa, PIWI and TDRKH were specifically immunolocalized in the germ cells of *P. reticulata*, with no specific signal detected in Sertoli cells and in other somatic cells of the gonad. These markers were detected in all stages of differentiation from early spermatogonia to advanced spermatids. Vasa staining was the strongest in spermatogonia, and then decreases throughout differentiation. Instead, both PIWI and TDRKH staining increases during differentiation, and their distribution pattern, similar to what observed in the mouse, suggests their concerted participation in the piRNA pathway also in this fish.

Keywords:

germline; spermatogenesis; *Poecilia reticulata*; Vasa; PIWI; TDRKH

Introduction

Spermatogenesis is the process of differentiation of germ cells that leads to the formation of male mature gametes. Spermatogenesis begins inside the testis with the mitotic proliferation of diploid spermatogonia, proceeds through the two meiotic divisions, and concludes with spermiogenesis, during which the haploid spermatids are transformed into spermatozoa (Schulz et al., 2010). In fish, spermatogenesis is of the "cystic type" (Schulz et al., 2010). Within the spermatogenic tubules, cyst formation initiates when cytoplasmic extensions of Sertoli cells envelope a single, clonally and synchronously developing group of germ cells deriving from a single spermatogonium (Grier et al., 2005). In *Poecilia reticulata*, the cysts containing spermatogonia in mitotic divisions are restricted to the testis periphery while the cysts containing germ cells in meiosis, migrate towards the region of the spermatic ducts (efferent ducts) located centrally in the testis, where spermiation occurs and where the cysts open to release spermatozoa (Parenti and Grier, 2004). Testis of *Poecilia reticulata* can be useful in studying the presence of germline determinants in spermatogenic cells because in each cyst germ cells are in the same developmental stage and this allows to easily analyze marker localization in specific germ cell stages. Germline determinants are components of germ granules both in females and in males (Saffman and Lasco, 1999). In male germ cells, these granules can then aggregate to form a chromatoid body (Parvinen, 2005). Later in spermiogenesis, at least in mammals, the chromatoid body appears like a ring adjacent to the midpiece and takes part in the formation of the residual body (Shang, 2010). Homologs of *vasa*, *piwi*, and *tudor* genes are an example of conserved genes expressed in germ granules, involved both in germline specification and in germ cell differentiation (Fierro-Constain et al., 2017; Juliano et al., 2010). Moreover, since they are expressed in germ cells (Juliano et al. 2010), they are used also to recognize germ cell localization (Cavelier et al., 2017; Cherif-Feildel et al., 2018). Vasa, an ATP-dependent RNA helicase belonging to the DEAD (Asp-Glu-Ala-Asp) box protein family, is a typical component of germ granules that promotes germline specification by regulating mRNA translation in germ cells during development (Seydoux and Braun, 2006). Vasa, given its precence from undifferentiated precursors to germ cells in advanced stages of differentiation, can be considered one of the best markers to trace germ cells (reviewed in Lasko, 2013). Vasa is conserved among metazoans (Linder et al. 1989) and it has been identified as germ cell determinant in several species, such as, for example: *Caenorhabditis elegans* (Gruidl et al., 1996), *Xenopus* (Ikenishi and Tanaka, 1997), *Danio rerio* (Yoon et al., 1997), *Podarcis sicula* (Maurizii et al., 2009; Milani and

Maurizii, 2014, 2015), chicken (Tsunekawa et al., 2000), mouse (Fujiwara et al., 1994), humans (Castrillon et al., 2000). A Vasa homolog was also characterized in the germ cells of the striped catfish (*Pangasianodon hypophthalmus*) (Duangkaew et al., 2019), and two Vasa isoforms have been identified in the male and female gonads of tilapia (*Oreochromis aureus*) (Kobayashi et al., 2002), and in medaka (*Oryzias latipes*) (Li et al., 2009; Reunov et al., 2020). The fundamental role of *vasa* for a proper gametogenesis has been pointed out with mutational experiments. In mice, male individuals carrying a mutation of the *vasa* ortholog *mvh* are sterile (Tanaka et al., 2000). In humans, loss of *vasa* leads to infertility with development of Sertoli cells only (Castrillon et al., 2000). In zebrafish, *vasa* loss-of-function mutations gave rise to sterile males that formed immature testes (Hartung et al., 2014).

PIWI proteins are other conserved components of germ granules and are essential for germline development and gametogenesis in animals (Thomson and Lin, 2009). PIWI proteins, together with PIWI-interacting RNAs (piRNA, generally 26–31 nucleotides in length), forms PIWI-piRNA complexes, which are involved in transposon silencing, protecting genome integrity during germ cell development, and also regulate translation, and guide epigenetic programming in the germline (Kim, 2006; Kim et al., 2009; Juliano et al., 2011). Animals lacking piRNAs exhibit activation of transposable elements (TEs) and defects in gametogenesis (Carmell et al., 2007). In mammals, PIWI proteins were found to be male specific (Bak et al., 2011). In mice, there are three members of PIWI-like proteins (PIWI), MILI (PIWI2), MIWI (PIWI1) and MIWI2 (PIWI4), and mutations in any one of these PIWI genes in the mouse caused spermatogenic arrest and ultimately resulted in male sterility (Deng and Lin, 2002; Kuramochi-Miyagawa et al., 2001, 2004; Carmell et al., 2007). In zebrafish, the two described PIWI proteins, Ziwi (PIWI1) and Zili (PIWI2) are expressed in both the male and female gonads (Tan et al., 2002; Houwing et al., 2008). Loss of Ziwi led to germ cell apoptosis, while Zili was essential for germ cell meiosis and differentiation (Houwing et al., 2007; 2008). *piwi* homologous genes have been reported also in other species of teleosts, such as the common carp (*Cyprinus carpio*), Nile tilapia (*Oreochromis niloticus*), half-smooth tongue sole (*Cynoglossus semilaevis*), turbot (*Scophthalmus maximus*), and dark sleeper (*Odontobutis potamophila*), in which PIWI proteins are considered to play an important role in gonadal development and gametogenesis (Zhou et al., 2012; Xiao et al., 2013; Zhang et al., 2014; Wang et al., 2017, 2018; Zhao et al., 2018).

Other factors involved in the piRNA pathway have also been identified in animals (Ishizu et al., 2012). TDRD proteins (Tudor domain-containing proteins) are known to interact with PIWI proteins by binding to symmetrically dimethylated arginine residues in the N-terminus of PIWI1 and PIWI2 in both mouse and zebrafish (Kirino et al., 2009; Reuter et al., 2009; Vagin et al. 2009).

TDRKH (also named TDRD2) is a protein containing Tudor and K homology (KH) domains (Zhang et al., 2017) required for spermatogenesis and involved in piRNA biogenesis. Specifically, in mice, TDRKH interacts directly with PIWI proteins (PIWI-like protein 1 (PIWI1), PIWI2, and PIWI4) (Chen et al., 2009; Vagin et al., 2009). In mice, TDRD2/TDRKH was identified as a component of the MIWI complex (Chen et al., 2009) involved in primary piRNA biogenesis pathway. Mutation of *tdrkh* results in male sterility due to meiotic defects with concurrent loss of retrotransposon silencing (Saxe et al., 2013).

In this study, we analyzed the immunolocalization of the three germline determinants Vasa, PIWI and TDRKH in *Poecilia reticulata* male germ cells to document their distribution pattern in the different stages of their differentiation, knowledge that at the moment is limited to a few species studied with the use of few molecular markers. To do this, we first verified with Western Blot the possibility to confidently use antibodies developed against protein homologs of other animals (e.g. anti-human PIWI and TDRKH) in this fish, then with anti-Vasa and nuclear staining, and the use of the confocal microscope, we identified male germ cells in different stage of differentiation. This allowed us to describe and compare the distribution pattern of the piRNA pathway proteins PIWI and TDRKH in the different germ cell stages. When possible, we compared our findings with what observed in other fish, otherwise we compared them with what documented in other model animals. Indeed, this is the first study on TDRKH distribution in fish. *Poecilia reticulata* is an important model system for biomonitoring and toxicological studies (Kinnberg et al., 2003; Antunes et al., 2017; Souza Trigueiro et al., 2021), making the acquisition of details on its development and cell lineage differentiation of basic importance (e.g. Bettini et al., 2012; Bettini et al., 2017). Moreover, given the described characteristics of its gonad, it could become a useful model system also to study germline development and differentiation.

Material and Methods

Experimental animals

In this study, twenty sexually mature males of *Poecilia reticulata* were used: six for immunohistochemistry (two animals for each antibody used), six for immunofluorescence (two animals for each antibody used), and eight for Western blot. Animals were purchased from a local aquarium shop (Bologna, Italy). Once in the lab, fish were immediately sacrificed by decapitation after being anaesthetized with 0.1% 3-aminobenzoic acid ethyl ester (MS-222, Sigma, St. Louis, MO). All procedures and experiments were conducted in accordance with the European guidelines for animal care.

SDS-PAGE

Testes of *P. reticulata* were removed from their abdominal cavity and homogenized using an Ultra Turrax T25 (Janke and Kunkel IKA-labortechnik) in a buffer containing 10mM Tris-HCl, pH 7.5, 1 mM ethylene glycol-bis(2-aminoethyl ether)-N,N,N',N'-tetraacetic acid (EGTA) and in the presence of the following protease inhibitors: 1 mM PMSF and 1 tablet of protease inhibitor cocktail (Complete Mini of Roche) in 5 mL of the buffer. Then samples were centrifuged at 7,500 xg for 10 minutes at 4°C. The supernatant was stored at -80°C.

We used different specimens for homogenization to avoid biased results due to individual variability in the germline differentiation stage. Proteins in the total homogenate were quantified using the Lowry method (Lowry et al., 1951). The same quantity of total proteins was loaded per lane (30 µg) and analyzed by SDS-PAGE (Sodium Dodecyl Sulphate-PolyAcrylamide Gel Electrophoresis) (Laemmli, 1970), using 8.5% acrylamide gels.

Protein sequence analyses and antibodies

We used ExPaSy (www.expasy.org) to infer the molecular weight (MW) of *P. reticulata* NCBI predicted proteins by using the Compute pI/MW tool (Gasteiger et al., 2005), and we used InterProScan (Finn et al., 2017) to recognize conserved protein domains in protein sequences. The used anti-Vasa was obtained against zebrafish Vasa (Table 1). For Piwi and TDRDKH detection, we used antibodies developed against the human protein. Anti-Piwi primary antibody was developed against human PIWI2 (NCBI: NP_060538). The primary antibodies used for TDRKH detection were both developed against of *Homo sapiens* (NP_001077432.1) orthologue (Table 1). We used T-Coffee (Notredame et al., 2000) (supplementary material) to align protein sequences of Vasa, PIWI and TDRKH from *P. reticulata* with the corresponding ortholog from the species used for antibody production (zebrafish, *Homo sapiens* and *Homo sapiens*, respectively).

Western Blot

For immunoblotting, proteins were transferred to a Hybond-ECL membrane (Amersham International, Buckinghamshire, UK). Non-specific protein-binding sites were blocked with 5% dried skimmed milk (Bio-Rad Laboratories, Hercules, CA, USA), 3% bovine serum albumin (BSA), 0.1% Tween 20 (Tw) (Sigma) in Tris Buffered Saline solution (TBS: 200 mM Trizma base; 137 mM NaCl), for 1 hour (hr) and 30 min, at room temperature (RT) and subsequently washed with TBS-0.1% Tw. Membranes were then incubated with the following primary antibodies developed in rabbit and diluted with TBS-0.1%Tw, pH 7.4: anti-Vasa antibody (Abcam), (1:

2,000); anti-Piwil2 (Abcam) (1:500), anti-TDRKH (Genetex) (1:1,000) overnight (ON) at 4°C and for 1 hr and 15 min at RT. After rinsing, the membranes were incubated with goat anti-rabbit secondary antibody, conjugate with horseradish peroxidase (HRP) (Santa Cruz Biotechnology Inc., Santa Cruz, CA, USA) at the dilution of 1:5,000 for 1 hr at RT. The washed membranes were treated with ECL Western Blotting Detection Reagents (GE Healthcare) and exposed to Hyperfilm ECL (GE Healthcare).

Immunoistochemistry (IHC)

Sample processing

Male gonads of *P. reticulata* were removed from their abdominal cavity and fixed in modified Bouin's solution containing a saturated aqueous solution of picric acid and formalin (ratio 3:1), for 24 hrs at room temperature. Picric acid was removed by prolonged washing in 0.1 M sodium phosphate buffer (PB), pH 7.4, at room temperature. Specimens were dehydrated in a graded series of ethanol (70, 80, 95, 100%, for 40 min each at RT) and subsequently embedded in Paraplast plus (Sherwood Medical, St. Louis, MO; melting point 55–57°C). Gonads were cut with a Leica RM2145 microtome and 5-µm-thick sections were mounted on silane-coated slides (Sigma) and dried. Adjacent slides were used for histochemical and immunohistochemical processing. For histochemical sample preparation, the entire body was processed with hematoxylin and eosin staining. Xylene deparaffinized sections were hydrated and stained with hematoxylin and eosin for the evaluation of testis morphology. Briefly, sections were stained with Carazzi's hematoxylin (Bio-Optica, Milano, I) for 10 min. Colour change was obtained with immersion in tap water for 5 min. The sections were then stained with aqueous 1% eosin Y solution (Bio-Optica) for 2 min. Excess eosin was removed with quick rinse in distilled water. After dehydration with ethanol solutions, sections were cleared with xylene and coverslipped with Permount (Fisher Scientific, Pittsburgh, PA).

Immunostaining

After sections deparaffinisation with xylene and rehydration, endogenous peroxidase activity was quenched with 1% H₂O₂ in 0.01 M Phosphate Buffer containing 0.15 M NaCl, pH 7.4, for 25 min. For antigen retrieval, tissue sections were immersed in 0.01 M citrate buffer, pH 6.0 and heated in a microwave oven (750 W) for two cycles of 5 min each at 98°C. Non-specific background staining was reduced by preincubation in PBS containing 10% normal goat serum (NGS; Vector Laboratories, Burlingame, CA), 1% bovine serum albumin (BSA; Sigma) and 0.1% Tween 20

(Merck, Darmstadt, Germany) for 30 min. Sections were incubated separately ON with the following primary antibodies in a moist chamber on a floating plate at 4 °C: the anti-Vasa antibody (Abcam), anti-Piwil2 (Abcam) and anti-TDRKH (Genetex), all produced in rabbit and diluted 1:200, 1:50, 1:50, respectively, in PBS containing 3% NGS, 1% BSA and 0.1% Tween 20. After rinsing in PBS with 0.1% Tween 20, the sections were incubated with HRP-conjugated goat anti-rabbit IgG (PI-1000, Vector Laboratories) diluted 1:100 in PBS containing 1% BSA and 0.1% Tween 20 for 1 hr at RT. After rinsing in PBS, immunoreaction was visualised using the intensified diaminobenzidine method (Adams, 1981). Sections were dehydrated in ethanol, cleared in xylene, and coverslipped with Permount (Fisher Scientific, Pittsburgh, PA). Finally, the slides were examined using an Olympus BH-2 microscope.

Immunofluorescence (IF)

Sample processing

Testes of adult *P. reticulata* were rapidly removed and fixed with 3.7% paraformaldehyde plus 0.25% or 0.5% glutaraldehyde (depending on gonads dimension) in a buffer containing 80mM KPIPES, 1mM MgCl₂, 5mM EGTA, and 0.2% Triton X-100 (Tx), pH 6.8, for 4 hrs at RT. Fixed testes were washed with phosphate-buffered saline (PBS) (128 mM NaCl, 2 mM KCl, 8 mM Na₂HPO₄, 2 mM KH₂PO₄), pH 7.2, for 1 hr, and embedded in 7% agar. Vibratome sections (Leica VT1000 S), were post-fixed with increasing concentrations of methanol (50–100%) and rehydrated in PBS or TBS (10 mM Tris–HCl, 155 mM NaCl), pH 7.4. Unreacted aldehydes were reduced with 70 mM sodium borohydride (NaBH₄) in TBS, pH 7.4, for 90 min at room temperature, followed by several washes with TBS-0.1%Tx for 2 hrs. Permeabilization was carried out by adding TBS-1%Tx to the sections and leaving the tissues ON at 4°C. Then, free-floating sections were processed for immunofluorescence as described below.

Immunostaining

Non-specific protein-binding sites were blocked in TBS-0.1%Tx containing 1% BSA, 10% normal goat serum (NGS; both from Sigma), pH 7.4 for 1 hr and 30 min at RT. As primary antibodies we used the following antibodies produced in rabbit and diluted with 3% BSA in TBS-0.1%Tx, pH 7.4: the anti-Vasa antibody (Abcam), diluted 1:200, anti-Piwil2 (Abcam) diluted 1:50 and anti-TDRKH (GeneTex), diluted 1:50, all incubated for 60 hrs at 4°C. After washing, the treated sections were incubated with a goat anti-rabbit polyclonal antibody, conjugated with Alexa Fluor 488, diluted 1:450 with 1% NGS and 1% BSA in TBS-0.1%Tx for 24 hrs at 4°C and then washed.

For alpha-Tubulin Immunostaining see Milani and Maurizii, 2015.

All the immunostained sections were stained with a nuclear dye, 1 μ M TO-PRO-3 iodide (Molecular Probes), in PBS, pH 7.2, for 10 min at RT and, after washing, mounted in 2.5% DABCO (1,4- diazabicyclo [2.2.2] octane (Sigma), 50 mM Tris), pH 8, 90% glycerol. Finally, the sections were covered with coverslips, sealed with nail polish and stored at 4°C, in the dark. Controls were performed using sections from which the first or the second antibody was replaced with 1% normal serum in TBS-0.1%Tx. Sections were examined with a Leica TCS SL confocal laser scanning microscope equipped with Ar/He/Ne lasers, employing Leica confocal software.

Results

Western blot

The anti-Vasa antibody detected a single strong band at about 70 kDa (Fig. 1), compatible with the expected MW (Table 1). A band of a molecular weight of about 78 kDa was detected with anti-Piwil2 (Fig. 1). Other very light bands of lower or higher MW were visible that can be due to nonspecific signal. For PIWI, the *P. reticulata* expected molecular weight was 116 kDa (Table 1), however if we consider only the functional domains (see Interproscan results; supplementary material) the weight would drop down considerably (up to ~67 kDa for the PAZ domain and the PIWI domain). About TDRKH, of the two isoforms, X1 was 32-AA longer in the N-terminus than X2. InterProScan (supplementary material) found that both the isoform X1 and X2 contain one KH1 and one TUDOR domains (Fig. 1), with the N terminus extension of X1 being not assigned to a specific functional domain. Anti-TDRKH GeneTex antibody detected a strong band compatible with a weight of 63 kDa (Fig. 1), corresponding to the expected weight of the heavier TDRKH isoform.

Histological organization of testis in *Poecilia reticulata*

Sections of testis of *P. reticulata* stained with haematoxylin and eosin (HE) show the tubular or “restricted type” organization of the single fused testis (Fig. 2). Cysts move from the periphery to the central region of the gonad where the efferent ducts reside (Fig. 2 a). Cysts containing germ cells in the early stages of spermatogenesis (spermatogonia and spermatocytes) are located near the periphery of the testis (Fig. 2 a). The region immediately beneath the apex of the testis shows cysts of different sizes containing spermatogonia (Fig. 2 b). Numerous and large cysts containing

spermatocytes are recognizable for their smaller size compared to that of spermatogonia (Fig. 2). It is difficult to distinguish cysts containing spermatocytes I from those containing spermatocytes II (Fig. 2). In any case, it must be considered that cysts containing spermatocytes II are seen less frequently than primary spermatocytes as they divide rapidly, after a short interphase between the 2 divisions of meiosis. Also, cysts containing only early spermatids are not easily seen (Fig. 2). In fact, spermatids are small cells, spherical in shape with a spherical nucleus with condensed chromatin, that rapidly undergo morphological transformation, becoming spermatozoa through the process called spermiogenesis. Differently, many cysts with numerous spermatids at different stages of spermiogenesis are located deeper, near the efferent ducts (Fig. 2 b, c). In the same region, peculiar cysts called “spermatozeugmata”, in which spermatozoa are tightly packed (Fig. 2 a, b, c), are also present. Spermatozeugmata show sperm heads oriented towards the Sertoli cells, while flagella are oriented towards the centre of the cyst (Fig. 2D, E). Spermatozeugmata are found also inside the efferent ducts where mature spermatozoa are finally released (Fig. 2 a, f).

Vasa Immunostaining

Anti-Vasa staining was performed on sections of *P. reticulata* testis and then Vasa localization pattern was utilized to trace germ cell localization and distribution inside the gonadic tissue.

IHC

A strong Vasa immunostaining is evident at the periphery of the testis, in cysts containing spermatogonia and spermatocytes (Fig. 3 a). In testis apical region, spermatogonia inside small cysts show a very strong Vasa staining in the cytoplasm (Fig. 3 b). Vasa appears also abundant in spermatocyte cytoplasm (Fig. 3 b). Furthermore, cysts containing spermatids show a progressively weaker immunostaining as they progress through spermiation (Fig. 3 a, c). In spermatozeugmata, the labelling results dashed and concentrated only at the edges of the cysts, where the sperm heads take contact with the Sertoli cells (Fig. 3 a, c).

IF

Vasa immunolocalization in testis sections of *P. reticulata* shows the labelling in all cysts containing germ cells at different stages of differentiation (Fig. 4 a). In the apical region, cysts of small size, each containing a generation of spermatogonia according to their different nuclear and cellular dimensions, are observed (Fig. 4 b). In spermatogonia, Vasa appears localized only in the cytoplasm, and particularly abundant to fill the entire cytoplasm. A stronger marking is present around the nucleus, where a deeply fluorescent ring is observed (Fig. 4 b). Unlabeled cells

positioned between spermatogonia and spermatocyte cysts are probably Sertoli cells not yet involved in cyst formation (Fig. 4 b). Also in spermatocytes I, Vasa immunolabeling appears cytoplasmatic with a granular distribution (Fig. 4 b). Aggregation of Vasa granules occurs gradually in the later stages of spermatogenesis as can be seen in the cytoplasm of spermatocytes II and early spermatids (Fig. 4 c). In early spermatids, Vasa aggregates forming a single, big spot located near the nucleus (Fig. 4 c inset). In spermatids at different stages of differentiation, Vasa marking is very weak with small, stained spots mainly localized in proximity of the nuclei (Fig. 4 c). The spermatozoa forming spermatozeugmata result unmarked; the labelling is present only at the periphery of the cysts, where sperm heads are in contact with Sertoli cells (Fig. 4 d).

PIWI immunostaining

IHC

A weak PIWI immunostaining is observed in spermatocytes inside the large cysts located in the apical region and in the spermatids in the different stages of differentiation inside cysts localized both in the periphery and deeper in the testis (Fig. 5 a, b). With this technique, spermatogonia inside small cysts, typically observed in the apex or in the peripheral region of the testis, result unmarked and consequently not recognizable (Fig. 5 a, b). Differently, the immunostaining is well evident in the cysts containing germ cells in the last stages of differentiation. In fact, a dashed marking is observed at the periphery of spermatozeugmata, where the heads of the spermatozoa make contact with the Sertoli cells (Fig. 5 b). Some spermatozeugmata show an additional ring of marking due to the spermatozoa reaching the peripheral region of the cysts (Fig. 5 a, b). Inside some efferent ducts, the peripheral region of spermatozeugmata results marked while in others it appears unmarked (Fig. c). In the former case, the wall of the efferent ducts results clearly immunostained (Fig. 5 c). Mature spermatozoa, after detachment from Sertoli cells, are released into the efferent ducts and appear clearly unmarked (Fig. 5 c).

IF

IF revealed the presence of the PIWI protein in all the cysts containing germ cells in differentiation, but, as shown in Fig. 6 a, the distribution pattern of this protein in germ cells varies in the different differentiation stages. In particular, in spermatogonia, inside small cyst, few labeled granules of the PIWI protein are detected in their cytoplasm; in spermatogonia observed inside a cyst of bigger size, the immunostained granules in their cytoplasm appear increased (Fig. 6 a). In spermatocytes, the presence of PIWI increases when compared to spermatogonia, and numerous marked granules are scattered in the cytoplasm (Fig. 6 a). In spermatocytes II, PIWI immunostained granules appear to aggregate in the cytoplasm forming bigger spots, while in spermatids a single large granule

appears located on one side of the nucleus (Fig. 6 a). In spermatzeugmata, a dotted marking is present at the periphery of the cysts, as observed with IHC (Fig. 6 b).

TDRKH Immunostaining

IHC

Anti-TDRKH antibody immunostaining is present in all the cysts that extend from the periphery to the central region of the testis (Fig. 7 a). At higher magnification, the peripheral region shows TDRKH protein in spermatogonia. In cysts containing spermatocytes, the immunostaining is weaker if compared to that of spermatogonia and appears with cytoplasmic localization (Fig. 7 a, b). Differently, the marking is clearly evident in the last stages of germ cells differentiation as for example, in cysts containing spermatids in spermiogenesis and in spermatzeugmata, where the immunolabelling is very strong in the peripheral region of the cysts (Fig. 7 b). The wall of some efferent ducts appears clearly immunostained, while the spermatzeugmata inside the efferent ducts results unmarked (Fig. 7 B).

IF

In the cysts containing spermatogonia and spermatocytes at the periphery of the testis TDRKH labeling is detected (Fig. 8 a). In particular, IF reveals that in spermatogonia the immunostained granules are few and scattered in the cytoplasm. In the spermatocytes I, the number of labelled granules increases considerably, and they fill the cytoplasm. In some areas of the cytoplasm, the granules coalesce to form larger aggregates (Fig. 8 a). TDRKH immunolabeling decreases in cysts containing germ cells in more advanced stages of spermatogenesis. In fact, cysts containing spermatocytes II and cysts containing spermatids at different stages of spermiogenesis, show a lower presence of TDRKH (Fig. 8 b). In particular, in the cytoplasm of spermatocytes II and in early spermatids present within the same cyst (Fig. 8 c), the immunostaining appears reduced but numerous granules are scattered in the cytoplasm. Also, a clear TDRKH labelling is observed in the peripheral region of cysts containing spermatzeugmata (Fig. 8 d).

Discussion

In this work we highlighted the immunolocalization and distribution pattern of three germline markers, i.e. Vasa, PIWI, and TDRKH proteins, in male germ cells of the fish *P. reticulata*. We used primary polyclonal antibodies in immunoistochemistry (IHC) and immunofluorescence (IF) assays after testing their specificity with Western Blot. To better understand the structural organization of *P. reticulata* testis, a histological study was conducted using sections of testis

stained with haematoxylin and eosin. Moreover, since the study of germline determinant localization requires a clear understanding of the different stages of germ cell differentiation, the nuclear dye TO-PRO3 was used at confocal laser scanning microscopy to clarify the differentiation stages of male germ cells during spermatogenesis.

Western blotting with anti-Vasa developed against Vasa zebrafish shows a single marked band of about 70-75 kDa, supporting its specificity. Also, this molecular weight corresponds to that documented for the marine medaka *Oryzias melastigma* (Reunov et al., 2020), and only a bit lighter than zebrafish Vasa homologue, which is around 80 kDa (Braat et al., 2000). Vasa molecular weight in these fish results comparable with that found for Vasa in the mouse *Mus musculus*, (MVH), where the molecular weight is around 85 kDa (Toyooka et al., 2000), and in humans, with a weigh of 79 kDa (Castrillon et al., 2000). Anti-Piwil2 antibody, developed against the human protein, detects a major band of about 78 kDa. The value is lower than the molecular weight of PIWI found in zebrafish (Houwing et al., 2007, 2008) and in the mouse (Deng and Lin, 2002). Anti-TDRKH developed against TDRKH protein of human shows a strong immunostained band almost matching the expected molecular weight of *P. reticulata* TDRKH protein (63.4 kDa the heaviest isoform). We did not find in bibliography an observed molecular weight for zebrafish TDRKH, however, Western blot analysis of mouse testis shows a highly marked band with anti-TDRKH with a molecular weight of approximately 70 kDa (Toyooka et al., 2000).

To identify germ cells within the testis of *P. reticulata*, we used Vasa as molecular marker given its wide spectrum of expression during germ line development (reviewed in Lasko, 2013).

Vasa immunolocalization is strongest in the peripheral cysts and it is present inside germ cells with a cytoplasmatic distribution, evident with both IHC and IF techniques. In particular, cysts containing mitotically dividing spermatogonia shows the strongest staining in respect to all other germ cells. With IF, we identified two different generations of spermatogonia (Fig. 4 b). The apical spermatogonia, with a large nucleus, appears to correspond to type A spermatogonia of mammals (Billard, 1984), and similar to other teleosts (Lofts 1968; Billard 1969), and to selachians (Stanley 1966; Holstein 1968). Instead, spermatogonia of smaller size and with a smaller nucleus (Fig. 4 b) appear homologous to type B spermatogonia of mammals that, differently to type A spermatogonia, do not mitotically divide but proceed with meiosis (Billard, 1984).

In spermatogonia and in spermatocytes, the Vasa staining appears granular with the numerous stained spots scattered in the cytoplasm (Fig. 4 b). Aggregation of Vasa granules occurs gradually in the later stages of spermatogenesis as can be seen in the cytoplasm of spermatocytes II and early spermatids (Fig. 4 c). In early spermatids, recognizable in IF for the round nucleus and compacted chromatin, Vasa protein aggregates forming a single big spot located near the nucleus (Fig. 4 c,

insert). Interestingly, this is similar to Vasa accumulation in the chromatoid body of mammals (Noce et al., 2001; Gustafson and Wessel, 2010), a structure present in sperm cells close to the end of their differentiation. In teleost fishes, the chromatoid body was found in some species, typically in the postmeiotic phase (Yuan et al., 2014 and references therein). However, in some fish, such as *P. reticulata*, no chromatoid body comparable to that of mammals has been described so far (Mattei and Mattei, 1978; Billard, 1983; Flores and Burns, 1993; Munoz et al., 2002). In this work, IF showed that spermatid cysts present a progressively weaker marking as they progress through spermiation. Indeed, late spermatids show only some stained spots, preferentially close to the elongated nucleus (Fig. 4 d), that probably represent immunostained Vasa contained in the cytoplasm of residual bodies.

In the spermatozeugmata, in which spermatozoa are tightly packed, a dashed staining is present only at the edge of the cyst, where the sperm heads are in contact with the Sertoli cells, as observed with both the assays (Figs 3 b and 4 d). This peculiar localization of Vasa immunostaining in spermatozeugmata is probably due to the disposal of the residual bodies of the late spermatids that contained Vasa protein in their cytoplasm (Grier, 1981; Uribe, 2014). In the testis of fish with “restricted type” organization, spermatozeugmata migrate towards the efferent ducts and, within them, mature spermatozoa are released, while the residual bodies are phagocytized by the Sertoli cells. After the detachment of spermatozoa, the Sertoli cells move to the periphery of the efferent duct, where they form the wall of the efferent duct (Grier, 1981; Uribe et al., 2014). According to this, in *P. reticulata* spermatozeugmata inside the efferent ducts, spermatozoa result unmarked after their detachment from the Sertoli cells (Fig. 3 b). The Sertoli cells appear unmarked in non-spermatozeugmata cyst; in addition, the confocal microscopy observations of small group of clearly unmarked Sertoli cells not yet organized into cysts reinforces this hypothesis (Fig. 4 b).

These findings together indicate that the Vasa protein can be used as a germline marker also in *P. reticulata*. Also, these results are in accordance with what already known in zebrafish (*Danio rerio*) (Baat et al., 2000) and in Gibel Carp (*Carassius auratus gibelio*) (Xu et al., 2005). The Vasa distribution pattern in *P. reticulata* appears exclusively cytoplasmatic, as found in other teleost fish such as zebrafish (Houwing et al., 2008) and Gibel Carp (*Carassius auratus gibelio*) (Xu et al., 2005). Also, in *P. reticulata*, Vasa immunostaining is present in spermatogonia, spermatocytes and early spermatids while no staining was detected in spermatozoa. In the Gibel Carp, Vasa was similarly present in spermatogonia but spermatocytes and spermatids show a low Vasa staining (Xu et al., 2005), while in *P. reticulata* Vasa was highly immunodetected also in spermatocytes. In tilapia (*Oreochromis niloticus*) testis, Vasa protein was localized in spermatogonia and in primary

spermatocytes but was not observed in secondary spermatocytes and spermatozoa (Kobayashi et al., 2002). This indicates for these fish a similar Vasa distribution pattern with modifications.

In zebrafish, *vasa* mutant gonads do not develop germ cells in the testis, that results empty and containing only somatic cells (Hartung et al., 2014). No data is yet available on the effects of *vasa* mutations in *P. reticulata* and functional analyses are necessary to verify its role in this species. In any case, the presence of Vasa protein in all the developmental stages suggests that it can have a role in the differentiation process of male germ cells during *P. reticulata* spermatogenesis.

In *P. reticulata*, PIWI is detected from early to later stages of spermatogenesis but absent in spermatozoa. However, IHC does not detect PIWI in spermatogonia in the apical region of the testis. This is probably due to the low presence of PIWI in spermatogonia, that was nonetheless detected in IF (Fig. 6 a). In more advanced spermatogonia, PIWI immunostaining increases, and the granules clearly appear with a cytoplasmic distribution.

In zebrafish, Zili (PIWII2) is found in cytoplasmic granules around spermatogonia and spermatocyte nuclei but is seen also in the nucleus showing a dynamic distribution between the two cell districts (Houwing et al. 2008); Zili is not detectable in later stages of zebrafish spermatogenesis. The same results were also observed in medaka (Li et al. 2012; Zhao et al. 2012).

In *P. reticulata* spermatocytes I, the presence of PIWI increases further and IF highlights the numerous immunostained granules scattered in the cytoplasm. In spermatocytes II, stained granules are aggregated forming bigger spots with a clear cytoplasmic distribution (Fig. 6 a). Therefore, in male germ cells of *P. reticulata*, PIWI localization appears only cytoplasmatic, no nuclear marking was observed in the analyzed stages.

In zebrafish, Ziwi (PIWII1) is detectable up to spermatids in the last stages of differentiation, with a predominant cytoplasmic distribution (Houwing et al., 2007). In the mouse, Miwi (PIWII1) is a cytoplasmic protein present only in the male germline from meiotic spermatocytes to elongating spermatids and *miwi* knockout is characterized by a block at the early spermatid stage (Deng and Lin, 2002). Also in zebrafish, *piwi* genes has a role in meiotic progression of developing sperm as shown by the use of mutants. In general, the role of PIWI-like proteins in meiosis appears to be conserved during evolution (Thomson and Lin, 2009). In *ziwi* mutant fish, for example, gametogenesis occurs but germ cells undergo increased apoptosis, resulting in loss of all germ cells by the time fish reach adulthood (Houwing et al., 2007) and *zili* null animals are agametic (Houwing et al., 2008).

In *P. reticulata* early spermatids, a single anti-PIWI-stained large granule appears located on one side of the nucleus (Fig 6 b), as seen in Vasa protein immunolocalization. In the mouse, MIWI has been localized to the chromatoid body (Kotaja and Sassone-Corsi, 2007). In zebrafish, germ-cell-

specific granules appear to be required for the regulation of translational activity in which the Piwi-like proteins appear to be involved (Houwing et al., 2007).

In *P. reticulata*, a weak PIWI immunostaining is observed also in elongated spermatids near the nuclei, probably representing immunostained PIWI inside the cytoplasm of residual bodies. Also Ziwi in zebrafish (Houwing et al., 2007), but also Miwi in the mouse (Deng and Lin, 2002), are present in late spermatids. In spermatocyte cysts of *P. reticulata*, a dashed and well evident marking is visible at the periphery of the cysts (Fig. 6 b). Moreover, within some spermatocyte cysts, an additional ring of Piwi immunostaining is present, probably due to late spermatids (or still immature sperm) reaching the peripheral region of the cysts (Fig. 5), where their heads make contact with the Sertoli cells while the flagella are oriented towards the center of the cyst (Fig. 5 b, f). The IHC analyses show that spermatozoa inside the efferent ducts are unmarked after their release from the Sertoli cells and that the Sertoli cells contribute to the duct wall formation (Fig. 3 c). Similar to what observed for Vasa, the staining observed at the periphery of spermatocyte cysts can depend by the presence of PIWI protein in the cytoplasm of the residual bodies of the late spermatids. In support of this, we did not observe staining in spermatocyte cysts after the detachment of the spermatozoa from the Sertoli cells, the staining is instead evident in the duct wall (Fig. 3 c). However, the wall of some efferent ducts results unmarked (Fig. 3 c), despite the presence inside them of spermatozoa already released by the Sertoli cells. This can be easily explained in the case of efferent ducts in which Sertoli cells have already phagocytized the residual bodies. In this regard, another aspect to consider is the asynchronous activity of the numerous efferent ducts present in fish testis (Grier, 1981), as also occurs in *P. reticulata* (Fig. 3 a, c). No PIWI signal is detected in Sertoli cells inside the cysts containing differentiating germ cells and in the somatic cells of the gonad, as also described in zebrafish (Houwing et al., 2007, 2008), and in the mouse (Deng and Lin, 2002).

Given the functions of TDRKH protein in germ cell maintenance and transposon silencing together with PIWI, we analyzed the immunolocalization pattern of TDRKH and its cellular distribution during *P. reticulata* spermatogenesis. TDRKH presence in the same differentiation stages as PIWI would have suggest a similar function in the germ cells of this fish.

In *P. reticulata* testis, both IHC and IF reveal TDRKH presence from spermatogonia to spermatids in advanced stages of spermiation, while spermatozoa resulted unmarked (Fig. 7 b). No data on TDRKH localization pattern in fish has been reported so far. In the mouse, immunofluorescence analyses detected TDRKH in spermatogonia, spermatocytes, and round spermatids, but not in elongating spermatids (Saxe et al., 2013). In *P. reticulata*, IHC detect strongly TDRKH protein in spermatogonia while a lower staining is present in spermatocytes and spermatids. In *P. reticulata*,

IF detects few TDRKH immunostained granules in the cytoplasm of early spermatogonia while the granules increase in the cytoplasm of more advanced spermatogonia inside larger cysts. This immunolocalization pattern of TDRKH is similar to that observed for PIWI, but different to what we documented for Vasa, which is highly immunostained also in early spermatogonia. In spermatocytes I, TDRKH granules increase further in number, and their distribution still appear only cytoplasmic, as no nuclear marking is observed in nuclei in all the stages of spermatogenesis analyzed. In the mouse, TDRKH staining is present in the cytoplasm of spermatogonia with a granular pattern and resulted particularly strong in meiotic primary spermatocytes, correlating with the onset of meiosis; in fact, *tdrkh*-null mutants show meiotic arrest at the zygotene stage (Saxe et al., 2013; Wang et al., 2020).

In *P. reticulata* spermatocytes II, IF detects numerous immunostained granules of TDRKH scattered in the cytoplasm and in the round spermatids many granules are visible as well (Fig. 8 c), similarly to what described in the mouse (Toyooka et al., 2000; Saxe, 2013). Indeed, in the mouse, TDRKH does not aggregate in the chromatoid body, but immunostained granules remain scattered in the cytoplasm (Ding et al., 2019; Wang et al., 2020). However, it has been demonstrated that TDRKH deficiency affects the localization of MIWI in the chromatoid body and spermiogenesis arrests (Meikar et al., 2014; Ding et al., 2019).

Thus, in *P. reticulata* testis, IHC detects a strong anti-TDRKH staining in spermatogonia, while a smaller amount is found in spermatocytes and spermatids. The TDRKH marking observed in elongated spermatids and close to spermatozoa, with both assays, can indicate the presence of the protein in the cytoplasm of residual bodies, as discussed for Vasa and PIWI.

TDRKH is immunodetected specifically in the germ cells of *P. reticulata* and no specific signal is detected in Sertoli cells and in the other somatic cells of the gonad supporting a germ cell-specific function of TDRKH as already observed in the mouse (Virant-Klun et al., 2016).

Conclusions

The results from the two assays used in this study (IF and IHC) are in accordance with each other, with the IF analyses at the confocal microscope allowing, as expected, the observation of a more detailed distribution pattern of the proteins in the cytoplasm of germ cells.

Vasa has the strongest staining in the cytoplasm of early spermatogonia, with the staining that decreases throughout differentiation, instead both PIWI and TDRKH staining increases during differentiation. Interestingly, Vasa and PIWI granules aggregate forming larger aggregates up to a single spot in spermatids, as observed in the mouse (Noce et al., 2001; Gustafson and Wessel, 2010;

Kotaja et al., 2006); instead, TDRKH granules are scattered in the cytoplasm and do not appear to aggregate in a single spot, similarly to what observed in the mouse (Ding et al., 2019; Wang et al., 2020). Immunolocalization of PIWI and TDRKH in the same stages of germ cell differentiation and with a distribution pattern similar to that observed in the mouse (Saxe et al., 2013) may suggest their concerted participation in the piRNA pathway also in this fish.

Author contributions

M.G.M. and L.M.: Conceptualization and Supervision; F.C. and M.I.: Formal analysis; L.M., F.C., M.I., M.L., V.F., M.G.M.: Investigation; L.M., M.L., V.F., M.G.M.: Resources; M.G.M.: Writing - Original Draft; All the authors: Writing - Review & Editing, and Visualization.

Availability of data and materials

Data and materials are available upon reasonable request. Address to M.G.M. (maria.maurizii@unibo.it) or L.M. (liliana.milani@unibo.it).

Conflict of interest

None.

Figure legends

Fig. 1. Western blot. WB with anti-Vasa, anti-PIWI and anti-TDRKH on *P. reticulata* total protein testis homogenate (30 µg). See table 1 for predicted molecular weights. Protein standard molecular weights on the left of each panel.

Fig. 2. Sections of *P. reticulata* testis stained with HE. **a** – The section shows the “Restricted type organization” of the testis. The cysts, from the periphery to the central region, contain germ cells in different stages of differentiation. In the central region of the testis, many efferent ducts are present (ED). **b** – Magnification of Figure 2a showing the cysts in different stages of differentiation containing, from the periphery to the central region of testis: spermatogonia (Sg), then spermatocytes (Sc) and spermatids at different stages of spermiation (St1, St2, St3). The cysts at more advanced phases of spermatogenesis, called spermatocyte (Sz), are positioned closer to the center of the testis. **c** – Magnification of the region showed in Figure 2b with cysts containing spermatids (st) and cysts containing spermatocyte (Sz) with different levels of organization of spermatozoa inside them. In larger spermatocyte, the sperm heads are oriented towards Sertoli

cells (SC) arranged at the periphery of the cysts, while flagella facing inwards; in smaller spermatocyte (SC), the sperm heads they are not all in contact with the Sertoli cells (SC). **d** – High magnification of a portion of spermatocyte (Sz) showing sperm heads in contact with the Sertoli cells (SC), and flagella oriented towards the inside of the cyst. **e** – High magnification of a portion of spermatocyte in which the TO-PRO-3 nuclear dye shows the sperm heads (in green) near the Sertoli cells (SC), while the anti-alpha tubulin stained the flagella (in red) extending towards the center of the cyst. **f** – Magnification of an efferent duct (ED) with inside many spermatocyte (Sz). In some of them, the spermatid heads are located in the proximity to Sertoli cells (arrow) while in others, the detachment of spermatozoa (*) from Sertoli cells are visible. [Sg: spermatogonia; Sc: spermatocytes; St: spermatids; Sz: spermatocyte; SC: Sertoli cells; ED: efferent ducts].

Fig. 3. Immunolocalization of Vasa on sections of *P. reticulata* testis by IHC. **a** – Immunostained section showing the labelling in the cysts that extend from the periphery to the central region of the section. A more evident marking is present in the cysts with germ cells in the early stages of differentiation (spermatogonia: Sg; spermatocytes: Sc) localized at the periphery of testis. **b** – Magnification of a portion of the section showed in Figure 3a in which spermatogonia (Sg) result strongly marked. An evident immunostaining is also observed in the cysts containing spermatocytes (Sc). **c** – A lower immunomarking is present in the cysts containing early spermatids (St), which is further reduced in those containing spermatids at more advanced stages of spermiation (St1; St2; St3). In spermatocyte (Sz), the labelling with anti-Vasa antibody is evident on the periphery of cysts (arrowheads) near Sertoli cells (SC) and appears as dashed labelling. [Sg: spermatogonia; Sc: spermatocytes; St: spermatids; Sz: spermatocyte; Sp: spermatozoa; SC: Sertoli cells].

Fig. 4. Immunolocalization of Vasa on sections of *P. reticulata* testis by IF. **a** – Section containing a portion of testis extended from the periphery to the central region. The immunolabeling is most evident in peripheral cysts. Vasa immunostaining is present in cysts containing germ cells at different stages of differentiation (spermatogonia: Sg; spermatocytes: Sc; spermatids: St1,2). **b** – Magnification of peripheral cysts showing a strong Vasa staining in spermatogonia (Sg) and spermatocytes (Sc). In particular, in spermatogonia (Sg1, Sg2) contained in the two small cysts, Vasa results very abundant and spread in their cytoplasm. A fluorescent ring is observed around the nucleus of spermatogonia (arrowheads). The group of unlabeled cells seen between spermatogonia and spermatocyte cysts are probably unmarked Sertoli cells (SC) not yet involved in cyst formation. In spermatocytes I (ScI), the cytoplasmatic Vasa immunolabeling appears with granular

distribution. **c** – Higher magnification of some cysts containing germ cells at different stages of differentiation. In spermatocytes II (Sc II) aggregation of Vasa granules occurs in the cytoplasm. In early spermatids (st), Vasa aggregates forming a single big spot (arrowhead) located near the nucleus (inset). In spermatids at advanced stages of differentiation (St3), small stained spots of Vasa localized mainly in proximity of the nuclei (arrowhead). **d** – In spermatogonia (Sg), Vasa immunostaining is detectable at cysts periphery (*), where sperm heads make contact with Sertoli cells. Inside spermatogonia (Sg) some sperm heads and small Vasa-stained spots are observed. [Sg: spermatogonia; Sc: spermatocytes; St: spermatids; Sz: spermatogonia; SC: Sertoli cells]. In red Vasa staining, in green TO-PRO-3 nuclear dye.

Fig. 5. Immunolocalization of Piwi on sections of *P. reticulata* testis by IHC. **a** –Section showing apical and central regions of the testis. A weak immunostaining is observed inside apical cysts containing spermatocytes (Sc). Cysts containing spermatogonia typically located in the peripheral region result unmarked. The peripheral region (*) of spermatogonia (Sz) shows a strong and dotted marking. In the central region many efferent ducts (ED) are present, with marked and unmarked spermatogonia inside. **b** – Magnification of a portion of testis showing a weak labeling in cysts containing spermatocytes and spermatids (spermatocytes: Sc; spermatids: St). The spermatogonia cysts (Sz) are at different stages of formation. In some spermatogonia, the immunostaining is present only at the periphery of the cyst (*) while in others an additional marked ring is observed inside the cyst (Arrowhead). **c** – Deep region of testis showing many efferent ducts (ED) with unmarked spermatogonia (Sz) inside. The wall of the efferent ducts shows evident marking (Arrows). [Sg: spermatogonia; Sc: spermatocytes; St: spermatids; Sz: spermatogonia; SC: Sertoli cells].

Fig. 6. Immunolocalization of PIWI on sections of *P. reticulata* testis by IF. **a** – PIWI localization in germ cells at different development stages. In spermatogonia inside small cyst (Sg1), few immunolabeled spots are visible in their cytoplasm; inside a bigger cyst, spermatogonia (Sg2) show an increased number of the immunostained granules in their cytoplasm. In spermatocytes I (Sc I), numerous marked granules are scattered in the cytoplasm. Bottom left, a portion of a cyst with spermatocytes II (ScII) showing numerous immunostained granules (see also inset). **b** – PIWI localization in germ cells at advanced stages of differentiation. In the inset, magnification of a portion of cyst containing early spermatids (St) with only a big spot near the nucleus (arrowhead). In spermatogonia (Sz), the dotted marking results at the periphery of the cysts (*). [Sg:

spermatogonia; Sc: spermatocytes; St: spermatids; Sz: spermatogonia; SC: Sertoli cells]. In magenta, anti-PIWI staining, in green TO-PRO-3 nuclear dye.

Fig. 7. Immunolocalization of TDRKH on sections of *P. reticulata* testis by IHC. **a** – Portion of section showing the labelling in cysts that extend from the periphery to the central region of the testis. A more evident marking is present in spermatogonia (Sg) contained in small cysts and in germ cells at more advanced stages of differentiation (Sz). In the central region, the wall of some efferent ducts (ED), transversely sectioned, is strongly marked. **b** – Portion of a section showing spermatogonia (Sg) and spermatocytes (Sc) clearly marked. A strong immunostaining is observed at the periphery (*) of spermatogonia (Sg). Inside the efferent ducts (ED) unmarked spermatogonia (Sg) are present. Wall portion of some efferent ducts results strongly immunostained (arrows). Below in the section, the large efferent duct (ED) shows unmarked wall. Inside, unmarked spermatogonia (Sg) are present. [Sg: spermatogonia; Sc: spermatocytes; St: spermatids; Sz: spermatogonia; SC: Sertoli cells; ED: efferent ducts].

Fig. 8. Immunolocalization of TDRKH on sections of *P. reticulata* testis by IF. **a** – TDRKH immunostaining in the cysts containing spermatogonia and spermatocytes at the periphery of the testis. Bottom right, spermatogonia (Sg) show few immunostained granules in the cytoplasm. In spermatocytes I (ScI), the labelled granules increase compared to spermatogonia and they fill the cytoplasm. In some areas of the cytoplasm, the granules coalesce to form larger aggregates (arrowhead). **b** – Cysts containing immunostained germ cells at different stages of differentiation: (Sg: spermatogonia; ScI: spermatocytes I; ScII: spermatocytes II; St: spermatids; Sz: spermatogonia). **c** – Portion of section showing cysts containing germ cells at advanced stage of differentiation. On the top, the large cyst contains both spermatocytes II (*) and spermatids (arrowhead). Inset: immunostained granules of TDRKH are visible in the cytoplasm of spermatocytes II (*) and round spermatids (arrowhead). **d** – In spermatids at advanced stage of spermiogenesis (St3), immunostained spots show a prevalent localization near the nucleus (see inset). In spermatogonia (Sg), the labelling is present in the peripheral region of the cyst (*) [Sg: spermatogonia; Sc: spermatocytes; St: spermatids; Sz: spermatogonia]. In red anti-TDRKH staining, in green TO-PRO-3 nuclear dye.

References

712 Antunes, A.M., Rocha, T. L., Pires, F.S., de Freitas, M.A., Milhomem Cruz Leite, V.R., Arana, S.,
 713 Moreira, P.C., Teixeira Saboia-Morais, S.M., 2017. Gender-specific histopathological
 714 response in guppies *Poecilia reticulata* exposed to glyphosate or its metabolite
 715 aminomethylphosphonic acid. *Applied Toxicology* 37, 1098-1107.
 716 Bak, C.W., Yoon, T.K., Choi, Y., 2011. Functions of PIWI proteins in spermatogenesis. *Clin. Exp.*
 717 *Reprod. Med.* 38, 61–67.
 718 Bettini, S., Lazzari, M., Franceschini, V., 2012. Quantitative analysis of crypt cell population during
 719 postnatal development of the olfactory organ of the guppy, *Poecilia reticulata* (Teleostei,
 720 Poeciliidae), from birth to sexual maturity. *J Exp Biol* 215, 2711–2715.
 721 Bettini, S., Milani, L., Lazzari, M., Maurizii, M.G., Franceschini, V., 2017. Crypt cell markers in
 722 the olfactory organ of *Poecilia reticulata*: analysis and comparison with the fish model
 723 *Danio rerio*. *Brain Structure and Function* 222, 3063–3074.
 724 Billard, R., 1983. Spermiogenesis in the rainbow trout (*Salmo gairdneri*); An ultrastructural study.
 725 *Cell Tissue Res.* 233, 265–84.
 726 Billard, R., 1984. Ultrastructural changes in the spermatogonia and spermatocyte of *Poecilia*
 727 *reticulata* during spermatogenesis. *Cell Tissue Res.* 237, 219-226.
 728 Billard, R., 1969. La spermatogenese du *Poecilia reticulata*. I -Estimation du nombre de
 729 générations goniales et rendement de la spermatogenèse. *Ann. Biol. Anita. Biochim.*
 730 *Biophys.* 9, 251–271.
 731 Braat, A.K., van de Water, S., Goos, H., Bogerd, J., Zivkovic, D., 2000. Vasa protein
 732 expression and localization in the zebrafish. *Mech. Dev.* 95, 271–274.
 733 Carmell, M.A., Girard, A., van de Kant, H.J., Bouchis, D., Bestor, T.H., de Rooij, D.G., Hannon,
 734 G.J., 2007. MIWI2 is essential for spermatogenesis and repression of transposons in the
 735 mouse male germline. *Dev. Cell* 12, 503–514.
 736 Castrillon, D.H., Quade, B.J., Wang, T.Y., Quigley, C., Crum, C.P., 2000. The human VASA gene
 737 is specifically expressed in the germ cell lineage. *Proc. Natl. Acad. Sci. USA* 97, 9585–
 738 9590.
 739 Cavelier, P., Cau, J., Morin, N., Delsert, C., 2017. Early gametogenesis in the Pacific oyster: new
 740 insights using stem cell and mitotic markers. *J. Exp. Biol.* 220, 3988–3996.
 741 Chen, C., Jin, J., James, D.A., Adams-Cioaba, M.A., Park, J.G., Guo, Y., Tenaglia, E., Xu, C., Gish,
 742 G., Min, J., Pawson, T., 2009. Mouse Piwi interactome identifies binding mechanism of
 743 Tdrkh Tudor domain to arginine methylated Miwi. *Proc. Natl. Acad. Sci. USA* 106, 20336–
 744 20341.

- Cherif-Feildel, M., Kellner, K., Goux, D., Elie, N., Adeline, B., Lelong, C., Berthelin, C.H., 2018. Morphological and molecular criteria allow the identification of putative germ stem cells in a lophotrochozoan, the Pacific oyster *Crassostrea gigas*. *Histochem. Cell Biol.* 151, 419–433.
- Deng, W., Lin, H., 2002. *miwi*, a murine homolog of *piwi*, encodes a cytoplasmic protein essential for spermatogenesis. *Dev. Cell* 2, 819–830.
- Ding, D., Liu, J., Dong, K., Melnick, A.F., Latham, K.E., Chen, C., 2019. Mitochondrial membrane-based initial separation of MIWI and MILI functions during pachytene piRNA biogenesis. *Nucleic Acids Res.* 47, 2594–2608.
- Duangkaew, R., Jangprai, A., Ichida, K., Yoshizaki, G., Boonanuntanasarn, S., 2019. Characterization and expression of *vasa* homolog in the gonads and primordial germ cells of the striped catfish (*Pangasianodon hypophthalmus*). *Theriogenology* 131, 61–71.
- Fierro-Constain, L., Schenkelaars, Q., Gazave, E., Haguenaue, A., Rocher, C., Ereskovsky, A., Borchiellini, C., Renard, E., 2017. The Conservation of the Germline Multipotency Program, from Sponges to Vertebrates: A Stepping Stone to Understanding the Somatic and Germline Origins. *Genome Biol. Evol.* 9, 474–488.
- Finn, R.D., Attwood, T.K., Babbitt, P.C., Bateman, A., Bork, P., Bridge, A. J., ..., Mitchell, A.L., 2017. InterPro in 2017-beyond protein family and domain annotations. *Nucleic Acids Research*, 45, D190–D199. <http://doi.org/10.1093/nar/gkw1107>
- Flores, J.A., Burns, J.R., 1993. Ultrastructural study of embryonic and early adult germ cells, and their support cells, in both sexes of *Xiphophorus* (Teleostei: Poeciliidae). *Cell Tissue Res.* 271, 263–70.
- Fujiwara, Y., Komiya, T., Kawabata, H., Sato, M., Fujimoto, H., Furusawa, M., Noce, T., 1994. Isolation of a DEAD-family protein gene that encodes a murine homolog of *Drosophila vasa* and its specific expression in germ cell lineage. *Proc. Natl. Acad. Sci. USA* 91, 12258–12262.
- Gasteiger, E., Hoogland, C., Gattiker, A., Duvaud, S., Wilkins, M.R., Appel, R.D., Bairoch, A., 2005. Protein Identification and Analysis Tools on the ExPASy Server; In John M. Walker (ed): *The Proteomics Protocols Handbook*, Humana Press. pp. 571-607.
- Souza Trigueiro, N.S., Gonçalves, B.B., Cirqueira Diaz, F., Celmade Oliveira Lima, E., Lopes Rocha, T., Teixeira Saboia-Morais, S.M., 2021. Co-exposure of iron oxide nanoparticles and glyphosate-based herbicide induces DNA damage and mutagenic effects in the guppy (*Poecilia reticulata*). *Environmental Toxicology and Pharmacology* 81, 103521.

778 Grier, H.J., Uribe, M.C., Parenti, L.R., De La Rosa-Cruz, G., 2005. Fecundity, the germinal
 779 epithelium, and folliculogenesis in viviparous fishes. In Uribe MC, Grier HJ. (Eds).
 780 Viviparous Fishes. New Life Publications Homestead, FL, USA. 2005. Pp:191–126.
 781 Grier, H.J., 1981. Cellular organization of the testis and spermatogenesis in fishes. Am. Zool. 21,
 782 345–357.
 783 Gruidl, M.E., Smith, P.A., Kuznicki, K.A., McCrone, J.S., Kirchner, J., Strome Roussell, D.L.,
 784 Bennett, K.L., 1996. Multiple potential germ-line helicases are components of the germ-
 785 line-specific P granules of *Caenorhabditis elegans*. Proc. Natl. Acad. Sci. USA 93, 13837–
 786 13842.
 787 Gustafson, E.A., Wessel, G.M., 2010. DEAD-box helicases: posttranslational regulation and
 788 function. Biochem. Biophys. Res. Commun. 395, 1–6.
 789 Hartung, O., Forbes, M.M., Marlow, L.F., 2014. Zebrafish vasa is required for germ-cell
 790 differentiation and maintenance. Mol. Reprod. Dev. 81, 946–961.
 791 Holstein AF (1968) Zur trage der lokalen Steuerung der Spermatogenese beim Dornhai (*Squalus*
 792 *acanthias* L.). Z. Zellforsch. 93, 265–281
 793 Houwing, S., Berezikov, E., Ketting, R.F., 2008. Zili is required for germ cell differentiation and
 794 meiosis in zebrafish. EMBO J. 27, 2702–2711.
 795 Houwing, S., Kamminga, L.M., Berezikov, E., Cronembold, D., Girard, A., van den Elst, H.,
 796 Filippov, D.V., Blaser, H., Raz, E., Moens, C.B., Plasterk, R.H.A., Hannon, G.J., Draper,
 797 B.W., Ketting, R.F., 2007. A role for Piwi and piRNAs in germ cell maintenance and
 798 transposon silencing in Zebrafish. Cell 129, 69–82.
 799 Ikenishi, K., Tanaka, T.S., 1997. Involvement of the protein of *Xenopus vasa* homolog (*Xenopus*
 800 *vasa*-like gene 1, XVLG1) in the differentiation of primordial germ cells. Dev. Growth
 801 Differ. 39, 625–633.
 802 Ishizu, H., Siomi, H., Siomi, M.C., 2012. Biology of PIWI-interacting RNAs: new insights into
 803 biogenesis and function inside and outside of germlines. Genes & Dev. 26, 2361–2373.
 804 Juliano, C., Wang, J., Lin, H., 2011. Uniting germline and stem cells: the function of Piwi proteins
 805 and the piRNA pathway in diverse organisms. Annu. Rev. Genet. 45, 447–469.
 806 Juliano, C.E., Swartz, S.Z., Wessel, G.M., 2010. A conserved germline multipotency program.
 807 Development 137, 4113–4126.
 808 Kim, V.N., 2006. Small RNAs just got bigger: Piwi-interacting RNAs (piRNAs) in mammalian
 809 testes. Genes Dev. 20, 1993–1997.

810 Kinnberg, K., Toft G., 2003. Effects of estrogenic and antiandrogenic compounds on the testis
811 structure of the adult guppy (*Poecilia reticulata*). *Ecotoxicology and Environmental Safety*
812 54, 16–24.

813 Kirino, Y., Kim, N., de Planell-Saguer, M., Khandros, E., Chiorean, S., Klein, P.S., Rigoutsos, I.,
814 Jongens, T.A., Mourelatos, Z., 2009. Arginine methylation of Piwi proteins catalysed by
815 dPRMT5 is required for Ago3 and Aub stability. *Nat. Cell Biol.* 11, 652–658.

816 Kobayashi, T., Kajiura-Kobayashi, H., Nagahama, Y., 2002. Two isoforms of *vasa* homologs in a
817 teleost fish: their differential expression during germ cell differentiation. *Mechanisms of*
818 *Development* 111, 167–171.

819 Kotaja, N., Sassone-Corsi, P., 2007. The chromatoid body: a germ-cell-specific RNA-processing
820 centre. *Nat. Rev. Mol. Cell Bio.* 8, 85–90.

821 Kotaja, N., Bhattacharyya, S.N., Jaskiewicz, L., Kimmins, S., Parvinen, M., Filipowicz, W.,
822 Sassone-Corsi, P., 2006. The chromatoid body of male germ cells: Similarity with
823 processing bodies and presence of Dicer and microRNA pathway components. *Proc. Natl.*
824 *Acad. Sci. USA* 103, 2647–2652.

825 Kuramochi-Miyagawa, S., Kimura, T., Yomogida, K., Kuroiwa, A., Tadokoro, Y., Fujita, Y., Sato,
826 M., Matsuda, Y., Nakano, T., 2001. Two mouse piwi-related genes: miwi and mili. *Mech.*
827 *Dev.* 108, 121–133.

828 Kuramochi-Miyagawa, S., Kimura, T., Ijiri, T.W., Isobe, T., Asada, N., Fujita, Y., Ikawa, M., Iwai,
829 N., Okabe, M., Deng, W., Lin, H., Matsuda, Y., Nakano, T., 2004. Mili, a mammalian
830 member of piwi family gene, is essential for spermatogenesis. *Development* 131, 839–849.

831 Laemmli, U.K., 1970. Cleavage of structural proteins during the assembly of the head of
832 bacteriophage T4. *Nature* 227, 680–685.

833 Lasko, P., 2013. The DEAD-box helicase vasa: evidence for a multiplicity of functions in RNA
834 processes and developmental biology. *Biochim. Biophys. Acta Gene Regul. Mech.* 1829,
835 810–816.

836 Li, M., Hong, N., Xu, H., Yi, M., Li, C., Gui, J., Hong, Y., 2009. *Medaka vasa* is required for
837 migration but not survival of primordial germ cells. *Mech. Dev.* 126, 366–381.

838 Li, M., Hong, N., Gui, J., Hong, Y., 2012. Medaka piwi is essential for primordial germ cell
839 migration. *Curr. Mol. Med.* 12, 1040–1049.

840 Linder, P., Lasko, P.F., Ashburner, M., Leroy, P., Nielsen, P.J., Nishi, K., Schnier, J., Slonimski,
841 P.P., 1989. Birth of the D-E-A-D box. *Nature* 337, 121–122.

842 Lofts, B., 1968. Patterns of testicular activity. In: Barrington E, Jorgensen CB (eds) *Perspectives in*
843 *endocrinology*. Acad Press London, New York, pp 236–304.

844 Lowry, O.H., Rosebrough, N.J., Farr, A.L., Randall, R., 1951. Protein measurement with the Folin
845 phenol reagent. *J. Biol. Chem.* 193, 265–275.

846 Mattei, C., Mattei, X., 1978. La spermiogenese d'un poisson teleosteen (*Lepadogaster*
847 *lepadogaster*). I. La spermatide. *Biol. Cell* 32, 257–66.

848 Maurizii, M.G., Cavaliere, V., Gamberi, C., Lasko, P., Gargiulo, G., Taddei, C., 2009. Vasa protein
849 is localized in the germ cells and in the oocyte-associated pyriform follicle cells during early
850 oogenesis in the lizard *Podarcis sicula*. *Dev. Genes Evol.* 219, 361–367.

851 Meikar, O., Vagin, V.V., Chalmel, F., Sostar, K., Lardenois, A., Hammell, M., Jin, Y., Da Ros, M.,
852 Wasik, K.A., Toppari, J. et al., 2014. An atlas of chromatoid body components. *RNA* 20,
853 483–495.

854 Milani L., Maurizii M.G., 2014. First evidence of Vasa expression in differentiating male germ
855 cells of a reptile. *Mol. Reprod. Dev.* 81, 678.

856 Milani L., Maurizii M.G., 2015. Vasa Expression in Spermatogenic Cells During the Reproductive-
857 cycle Phases of *Podarcis sicula* (Reptilia, Lacertidae). *J. Exp. Zool. (Mol. Dev. Evol.) J.*
858 324B, 424–434.

859 Munoz, M., Sàbat, M., Mallol, S., Casadevall, M., 2002. Gonadal structure and gametogenesis of
860 *Trigla lyra* (Pisces: Triglidae). *Zool. Stud.* 41, 412–20.

861 Noce, T., Okamoto-Ito, S., Tsunekawa, S., 2001. Vasa Homolog Genes in Mammalian Germ Cell
862 Development. *Cell Structure and Function* 26, 131–136.

863 Notredame, C., Higgins, D.G., Heringa, J., 2000. T-Coffee: A novel method for fast and accurate
864 multiple sequence alignment. *J. Mol. Biol.* 302, 205–17.

865 Parenti, L.R., Grier, H.J., 2004. Evolution and phylogeny of gonad morphology in bony fishes.
866 *Integr. Comp. Biol.* 44, 333–348.

867 Parvinen, M., 2005. The chromatoid body in spermatogenesis. *Int. J. Androl.* 28, 189–201.

868 Reunov, A.A., Au, D.W., Alexandrova, Y.N., Chiang, M.W., Wan, M.T., Yakovlev, K.V.,
869 Reunova, Y.A., Komkova, A.V., Cheung, N.K., Peterson, D.R., Adrianov, A.V., 2020.
870 Germ plasm-related structures in marine medaka gametogenesis; novel sites of Vasa
871 localization and the unique mechanism of germ plasm granule arising. *Zygote* 28, 9–23.

872 Reuter, M., Chuma, S., Tanaka, T., Franz, T., Stark, A., Pillai, R.S., 2009 Loss of the Mili-
873 interacting Tudor domain-containing protein-1 activates transposons and alters the Mili-
874 associated small RNA profile. *Nat. Struct. Mol. Biol.* 16, 639–46.

875 Saffman, E.E., Lasko, P., 1999. Germline development in vertebrates and invertebrates. *Cell Mol.*
876 *Life* 55, 1141–63.

877 Saxe, J.P., Chen, M., Zhao, H., Lin, H., 2013. Tdrkh is essential for spermatogenesis and
878 participates in primary piRNA biogenesis in the germline. *EMBO J.* 32, 1869–1885.

879 Schulz, R.W., Franca, L.R., Lareyre, J.-J., Le Gac, F., Chiarini-Garcias, H., Nobrega, R.H., Miura,
880 T., 2010. Spermatogenesis in Fish. *Gen. Comp. Endocrinol.* 165, 390–411.

881 Seydoux, G., Braun, R.E., 2006. Pathway to totipotency: lessons from germ cells. *Cell* 127, 891–
882 904.

883 Shang, P., Baarends, W.M., Hoogerbrugge, J., Ooms, M.P., van Cappellen, W.A., de Jong, A.A.,
884 Dohle, G.R., van Eenennaam, H., Gossen, J.A., Grootegoed, J.A., 2010. Functional
885 transformation of the chromatoid body in mouse spermatids requires testis-specific
886 serine/threonine kinases. *J. Cell Sci.* 123, 331–339.

887 Stanley, H.P., 1966. The structure and the development of the seminiferous follicle in *Scyliorhinus*
888 *caniculus* and *Torpedo marmorata* (Elasmobranchii). *Z. Zellforsch.* 75, 453–468.

889 Tan, C.H., Lee, T.C., Weeraratne, S.D., Korzh, V., Lim, T.M., Gong, Z., 2002. Ziwi, the zebrafish
890 homologue of the *Drosophila* piwi: co-localization with vasa at the embryonic genital ridge
891 and gonad-specific expression in the adults. *Mech. Dev.* 119, S221–S224.

892 Tanaka, S.S., Toyooka, Y., Akasu, R., Katoh-Fukui, Y., Nakahara, Y., Suzuki, R., Yokoyama, M.,
893 Noce, T., 2000. The mouse homolog of *Drosophila* Vasa is required for the development of
894 male germ cells. *Genes Dev.* 14, 841–853.

895 Thomson, T., Lin, H., 2009. The Biogenesis and Function of PIWI Proteins and piRNAs: Progress
896 and Prospect. *Annu. Rev. Cell Dev. Biol.* 25, 355–76.

897 Toyooka, Y., Tsunekawa, N., Takahashi, Y., Matsui, Y., Satoh, M., Noce, T., 2000.
898 Expression and intracellular localization of mouse Vasa-homologue protein during germ cell
899 development. *Mech Dev.* 93, 139–49. doi: 10.1016/s0925-4773(00)00283-5.

900 Tsunekawa, N., Naito, M., Sakai, Y., Nishida, T., Noce, T., 2000. Isolation of chicken vasa
901 homolog gene and tracing the origin of primordial germ cells. *Development* 127, 2741–
902 2750.

903 Uribe, M.C., Grier, H.J., Mehjía-Roa, V., 2014. Comparative testicular structure and
904 spermatogenesis in bony fishes. *Spermatogenesis* 4, e983400.

905 Vagin, V.V., Wohlschlegel, J., Qu, J., Jonsson, Z., Huang, X., Chuma, S., Girard, A.,
906 Sachidanandam, R., Hannon, G.J., Aravin, A.A., 2009, Proteomic analysis of murine Piwi
907 proteins reveals a role for arginine methylation in specifying interaction with Tudor family
908 members. *Genes Dev.* 23, 1749–1762.

909 Virant-Klun, I., Leicht, S., Hughes, C., Krijgsveld, J., 2016. Identification of Maturation-Specific

910 Proteins by Single-Cell Proteomics of Human Oocytes. *Mol. Cell Proteomics* 15, 2616–
 911 2627.

912 Wang, X., Lv, C., Guo, Y., Yuan, S., 2020. Mitochondria Associated Germinal Structures in
 913 Spermatogenesis: piRNA Pathway Regulation and Beyond. *Cells* 9, 399.

914 Wang, H., Wang, B., Liu, J., Li, A., Zhu, H., Wang, X., Zhang, Q., 2018. *Piwill* gene is regulated
 915 by hypothalamic-pituitary-gonadal axis in turbot (*Scophthalmus maximus*): a different effect
 916 in ovaries and testes. *Gene* 658, 86–95.

917 Wang, H., Wang, B., Liu, X., Liu, Y., Du, X., Zhang, Q., Wang, X., 2017. Identification and
 918 expression of *piwil2* in turbot *scophthalmus maximus*, with implications of the involvement
 919 in embryonic and gonadal development. *Comp. Biochem. Physiol. B Biochem. Mol. Biol.*
 920 208–209, 84–93.

921 Xiao, J., Zhou, Y., Luo, Y., Zhong, H., Huang, Y., Zhang, Y., Luo, Z., Ling, Z., Zhang, M., Gan,
 922 X., 2013. Suppression effect of LHRH-A and hCG on Piwi expression in testis of Nile
 923 tilapia *Oreochromis niloticus*. *Gen. Comp. Endocrinol.* 189, 43–50.

924 Xu, H., Gui, J., Hong, Y., 2005. Differential Expression of vasa RNA and Protein During
 925 Spermatogenesis and Oogenesis in the Gibel Carp (*Carassius auratus gibelio*), a Bisexually
 926 and Gynogenetically Reproducing Vertebrate. *Dev. Dyn.* 233, 872–882.

927 Yoon, C., Kawakami, K., Hopkins, N., 1997. Zebrafish vasa homologue RNA is localized to the
 928 cleavage planes of 2- and 4-cell-stage embryos and is expressed in primordial germ cells.
 929 *Development* 124, 3157–3166.

930 Yuan, Y., Li, M., Hong, Y., 2014. Light and electron microscopic analyses of Vasa expression in
 931 adult germ cells of the fish medaka. *Gene* 545, 15–22.

932 Zhang, L., Liu, W., Shao, C., Zhang, N., Li, H., Liu, K., Dong, Z., Qi, Q., Zhao, W., Chen, S.,
 933 2014. Cloning, expression and methylation analysis of *piwil2* in half-smooth tongue sole
 934 (*Cynoglossus semilaevis*). *Mar. Genom.* 18, 45–54.

935 Zhang, H., Liu, K., Izumi, N., Huang, H., Ding, D., Ni, Z., Sidhu, S.S., Chen, C., Tomari, Y., Min,
 936 J., 2017. Structural basis for arginine methylation-independent recognition of PIWIL1 by
 937 TDRD2. *Proc. Natl. Acad. Sci. USA* 114, 12483–12488.

938 Zhao, H., Duan J., Cheng N, Nagahama Y., 2012. Specific expression of Olpiwi1 and Olpiwi2 in
 939 medaka (*Oryzias latipes*) germ cells. *Biochemical and Biophysical Research*
 940 *Communications* 418, 592–597.

941 Zhao, C., Zhu, W., Yin, S., Cao, Q., Zhang, H., Wen, X., Zhang, G., Xie, W., Chen, S., 2018.
 942 Molecular characterization and expression of *Piwill* and *Piwil2* during gonadal development
 943 and treatment with HCG and LHRH-A2 in *Odontobutis potamophila*. *Gene* 647, 181–191.

Zhou, Y., Wang, F., Liu, S., Zhong, H., Liu, Z., Tao, M., Zhang, C., Liu Y., 2012.
Human chorionic gonadotropin suppresses expression of Piwis in common
carp (*Cyprinus carpio*) ovaries. Gen. Comp. Endocrinol. 176, 126-131.

Table 1. Predicted and observed (WB) protein molecular weight and list of primary antibodies used.

Predicted protein [<i>Poecilia reticulata</i>]	NCBI	MW predicted
ATP-dependent RNA helicase DDX4	XP_008428196.1	70 kDa
Piwi-like protein 2	XP_008415818.1	116 kDa
Tudor and KH domain-containing protein	XP_008436386.1 (isoform X1)	63.4 kDa
	XP_008436387.1 (isoform X2)	59.9 kDa
	Ab1	MW observed
Anti-VASA	Abcam, ab209710 (1:2,000)	~ as predicted
Anti-PIWI2	Abcam, ab98852 (1:500)	~ 78 kDa
Anti-TDRKH	GeneTex, GTX129795 (1:1,000)	~ as predicted

Note: ExPaSy (www.expasy.org) predicted the molecular weight (MW) of the analyzed proteins.

Figure 1

[Click here to access/download;Figure;Fig1.png](#)

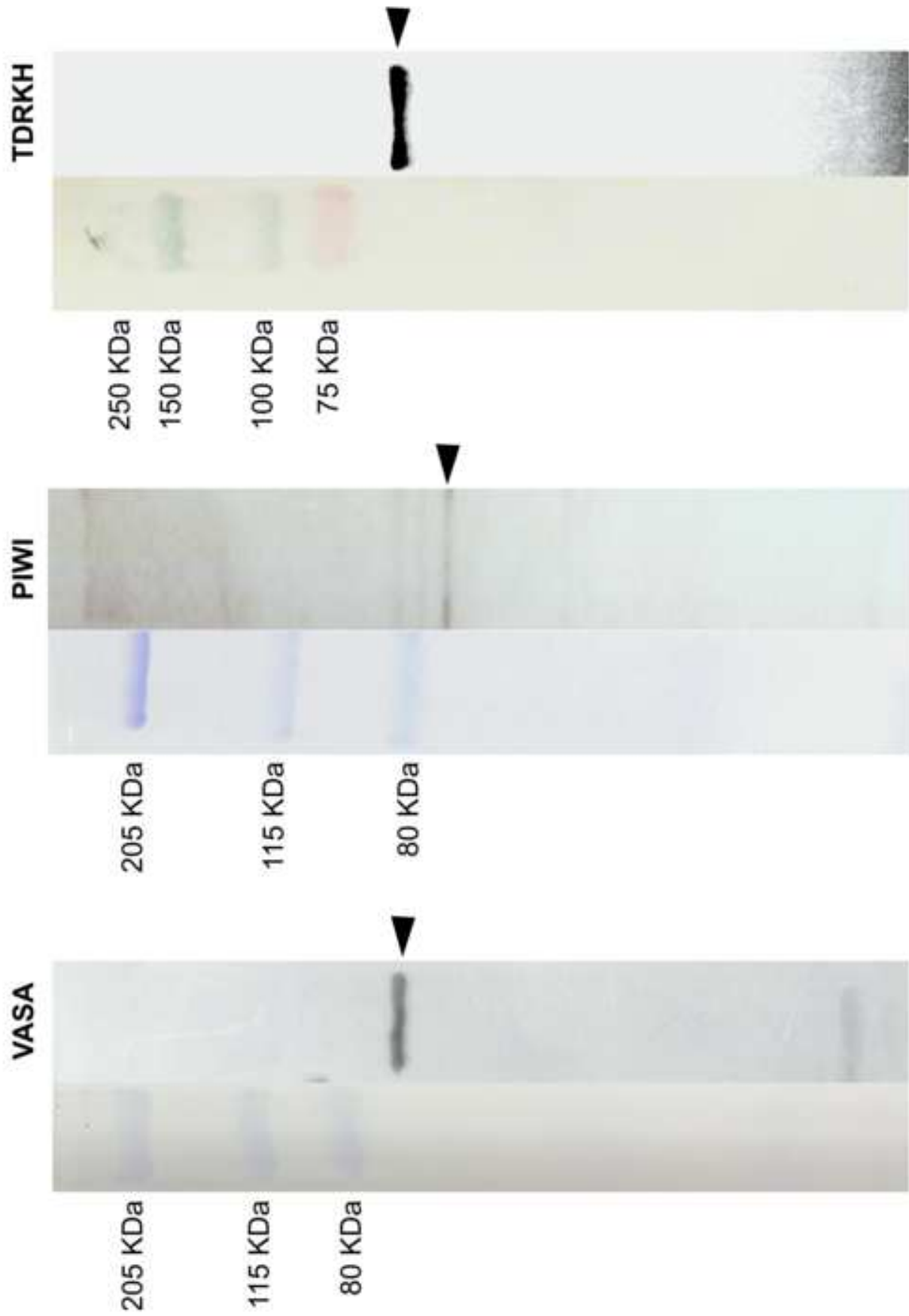


Figure 2

[Click here to access/download;Figure;Fig2.png](#)

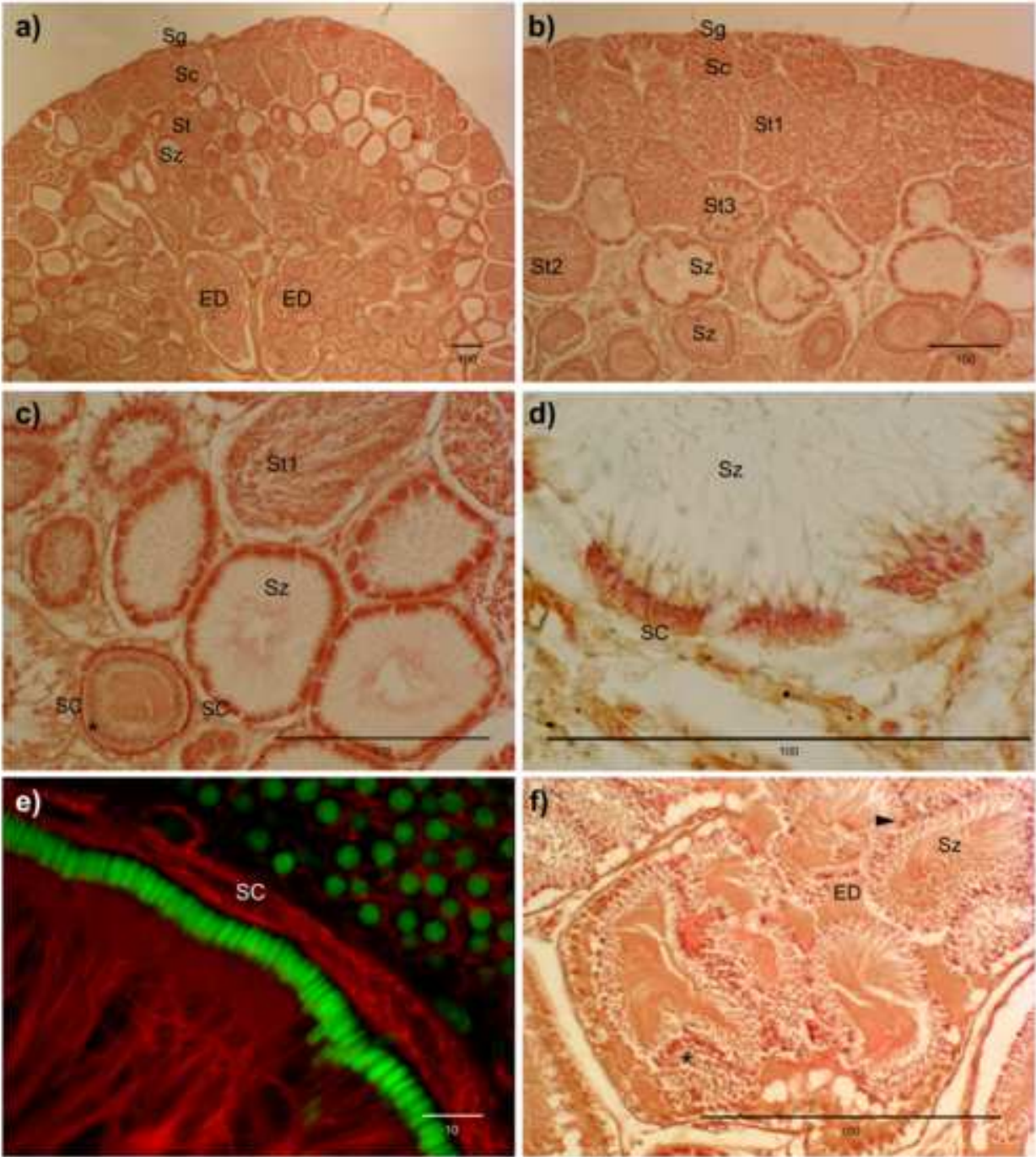


Figure 3

[Click here to access/download;Figure;Fig3.png](#)

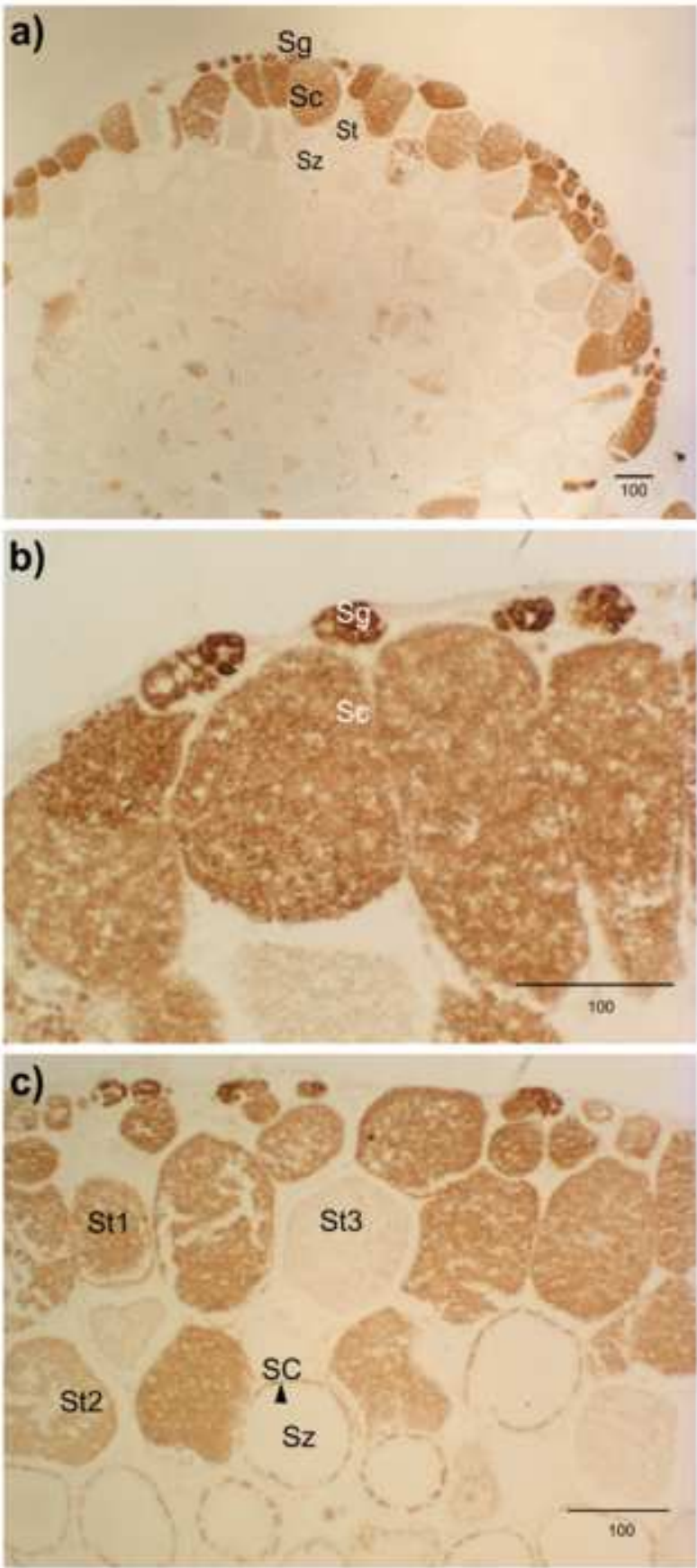


Figure 4

[Click here to access/download;Figure;Fig4.png](#)

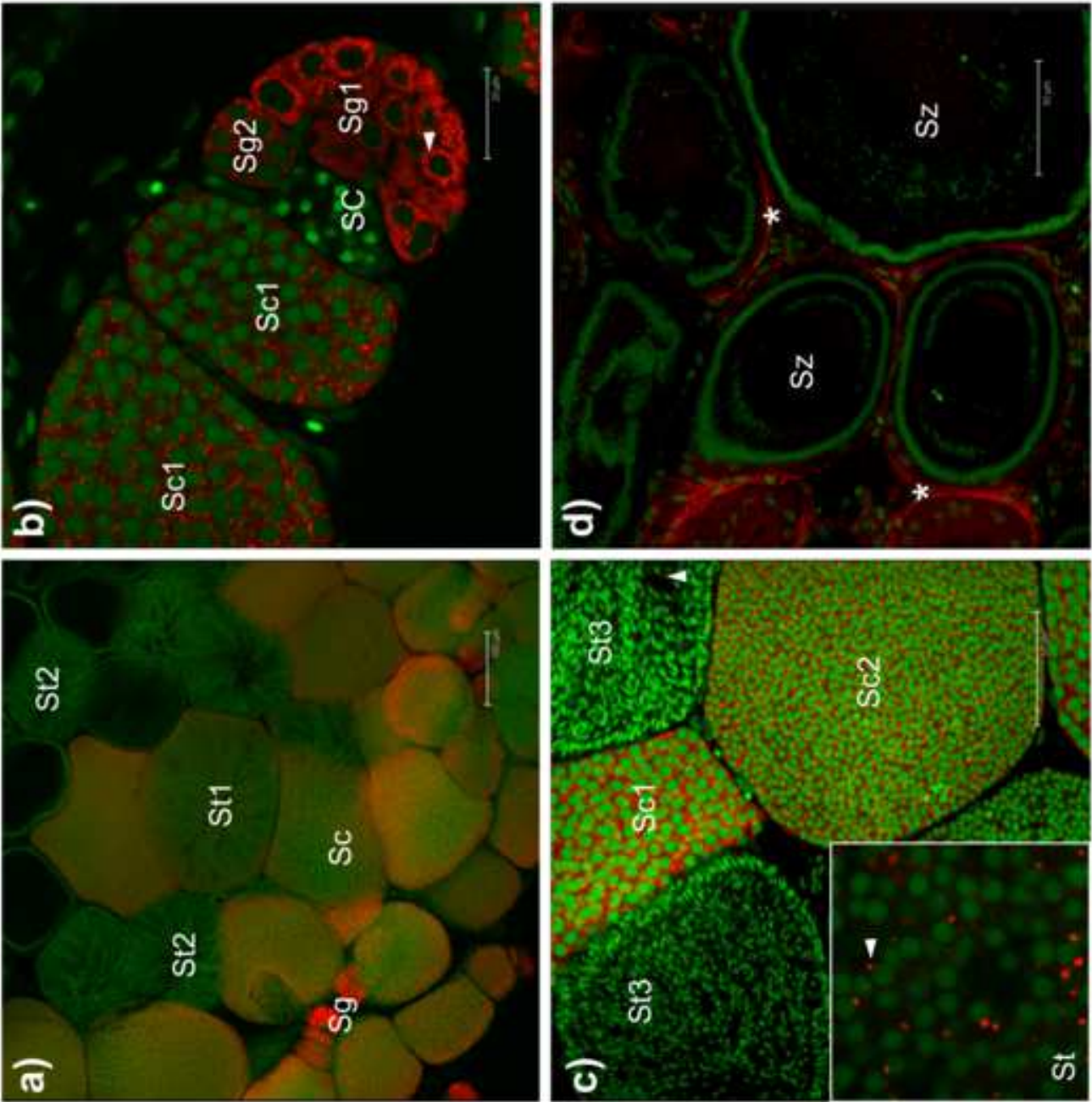


Figure 5

[Click here to access/download;Figure;Fig5.png](#)

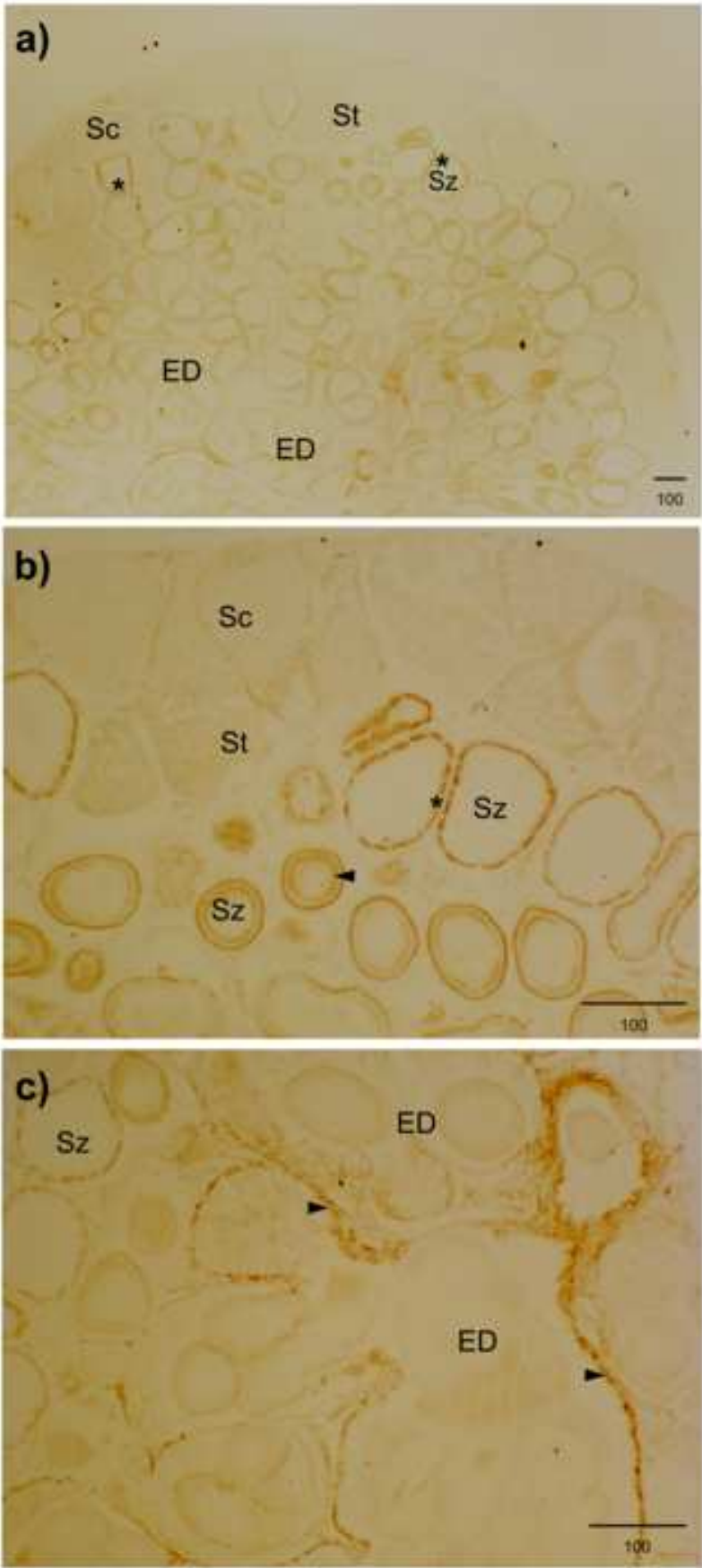


Figure 6

[Click here to access/download;Figure;Fig6.png](#)

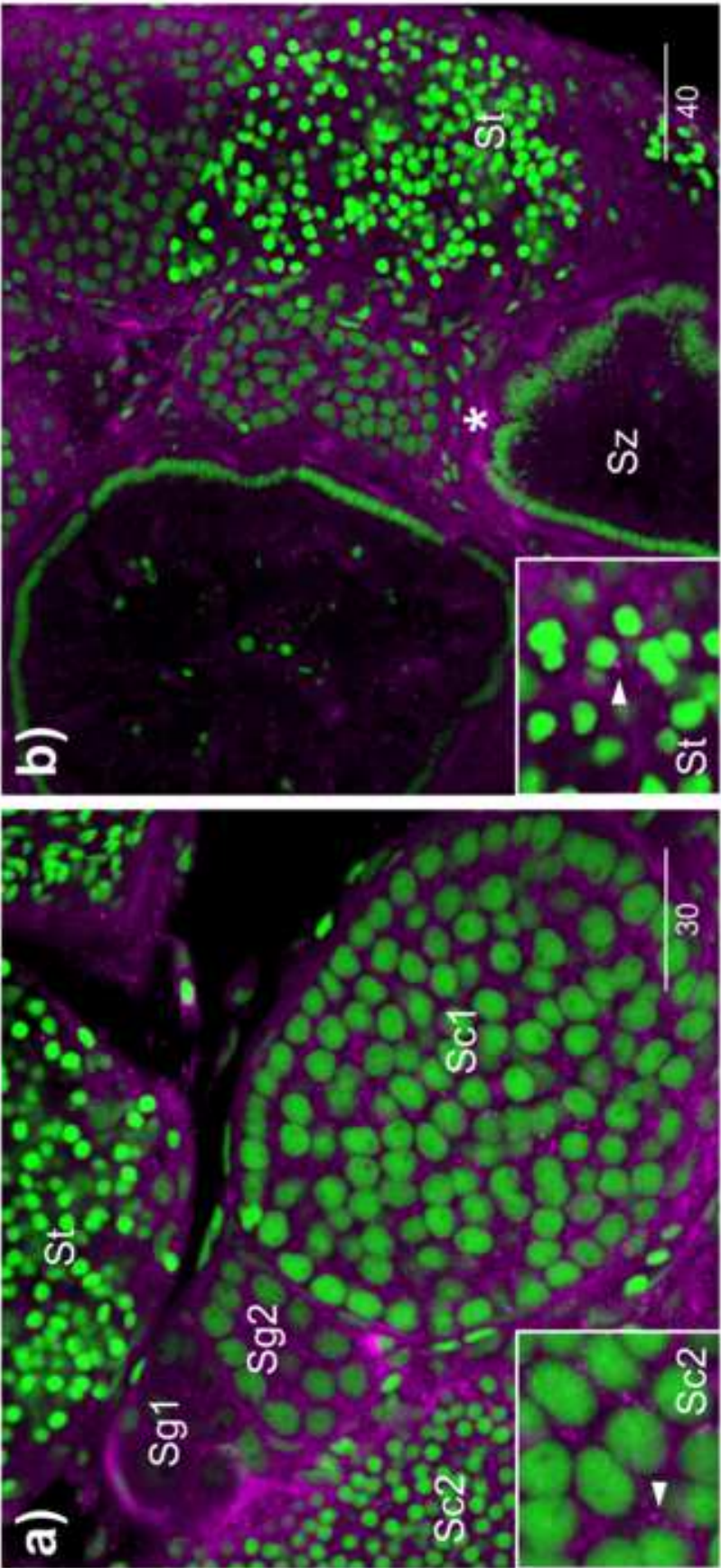


Figure 7

[Click here to access/download;Figure;Fig7.png](#)

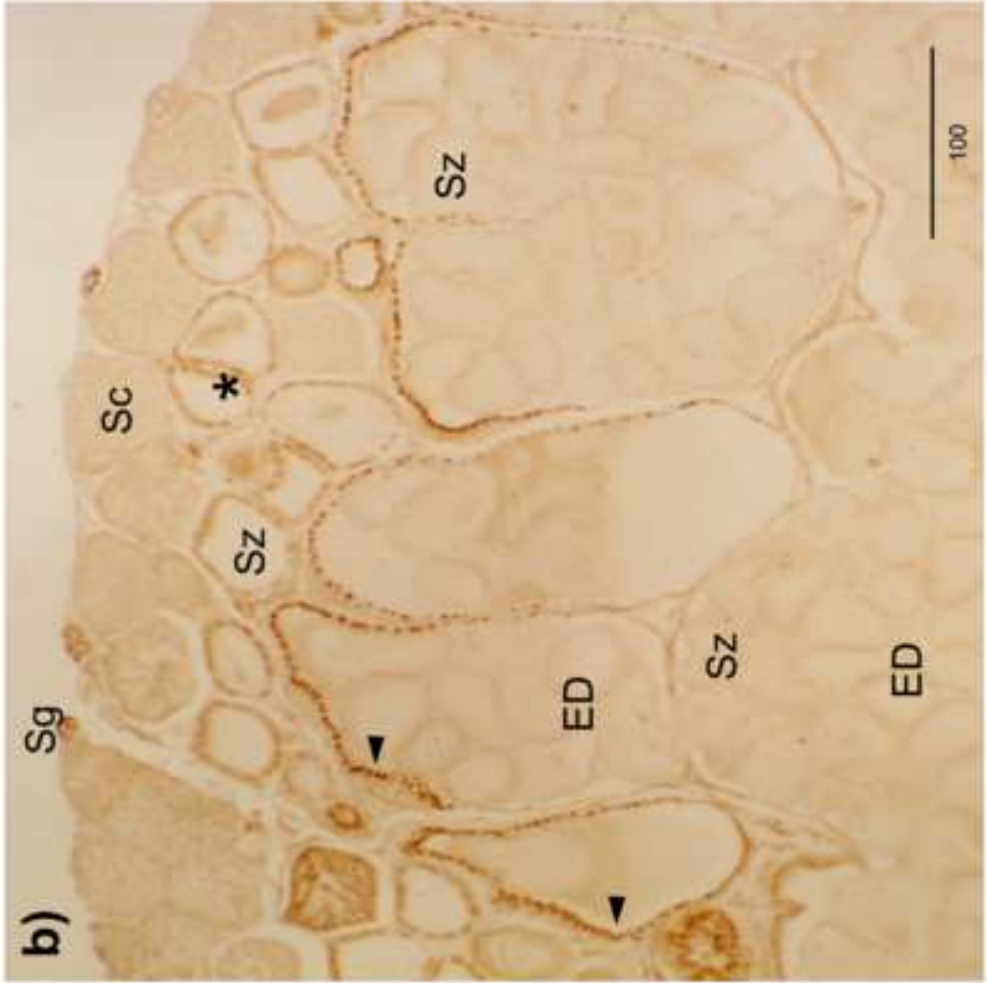
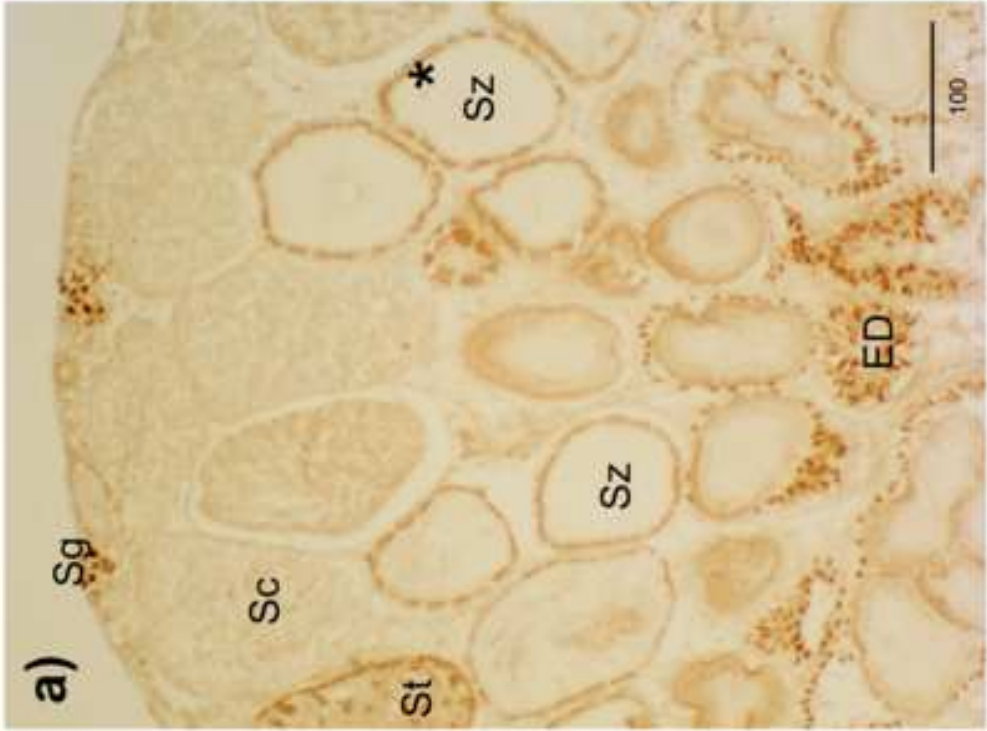
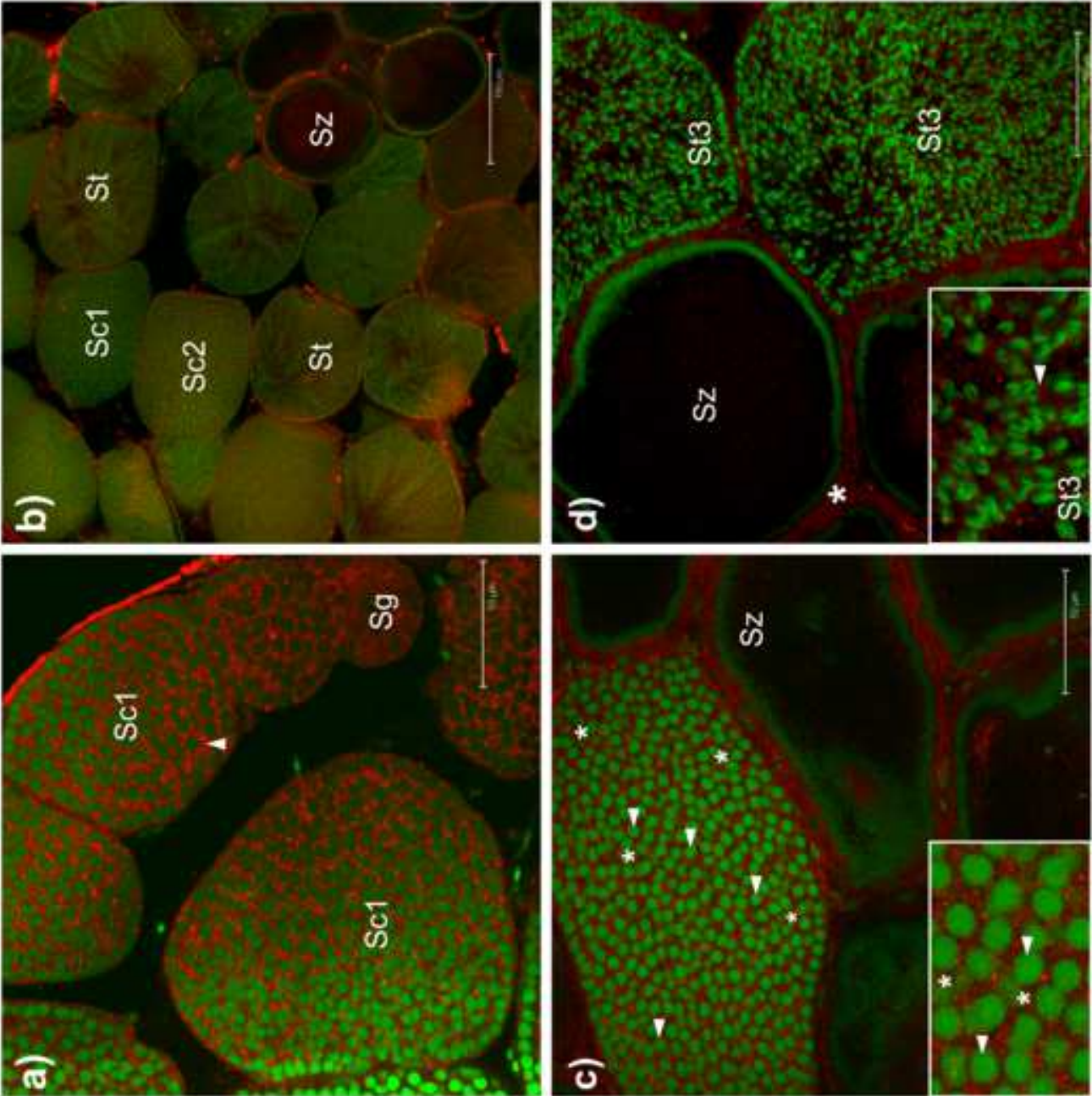


Figure 8

[Click here to access/download;Figure;Fig8.png](#)



Supplementary Materials

	Analysis	Signature accession	Signature description	Start	Stop	e-value	InterPro accession	InterPro description
XP_008428196.1 ATP-dependent RNA helicase DDX4 [Poecilia reticulata]	MobiDBLite	mobidb-lite	consensus disorder prediction	1	174	-	-	-
	ProSitePatterns	PS00039	DEAD-box subfamily ATP-dependent helicases signature.	362	370	-	IPR000629	ATP-dependent RNA helicase DEAD-box, conserved site
	PANTHER	PTHR47958:SF11	ATP-DEPENDENT RNA HELICASE DDX4-RELATED	74	598	0	-	-
	SMART	SM00490	helicmild6	472	553	8.30E-35	IPR001650	Helicase, C-terminal
	MobiDBLite	mobidb-lite	consensus disorder prediction	93	108	-	-	-
	Pfam	PF00271	Helicase conserved C-terminal domain	445	553	4.00E-31	IPR001650	Helicase, C-terminal
	MobiDBLite	mobidb-lite	consensus disorder prediction	27	43	-	-	-
	PANTHER	PTHR47958	ATP-DEPENDENT RNA HELICASE DBP3	74	598	0	-	-
	ProSiteProfiles	PSS1195	DEAD-box RNA helicase Q motif profile.	206	234	11.11268	IPR014014	RNA helicase, DEAD-box type, Q motif
	MobiDBLite	mobidb-lite	consensus disorder prediction	59	75	-	-	-
	Pfam	PF00270	DEAD/DEAH box helicase	230	408	3.50E-50	IPR011545	DEAD/DEAH box helicase domain
	Gene3D	G3DSA:3.40.50.300	-	426	597	7.70E-56	IPR027417	P-loop containing nucleoside triphosphate hydrolase
	ProSiteProfiles	PSS1194	Superfamilies 1 and 2 helicase C-terminal domain profile.	448	593	24.3666	IPR001650	Helicase, C-terminal
	MobiDBLite	mobidb-lite	consensus disorder prediction	594	639	-	-	-
	MobiDBLite	mobidb-lite	consensus disorder prediction	132	160	-	-	-
	ProSiteProfiles	PSS1192	Superfamilies 1 and 2 helicase ATP-binding type-1 domain profile.	237	420	31.82966	IPR014001	Helicase superfamily 1/2, ATP-binding domain
	CDD	cd18787	SF2_C_DEAD	433	562	7.05E-60	-	-
	Gene3D	G3DSA:3.40.50.300	-	168	424	2.40E-81	IPR027417	P-loop containing nucleoside triphosphate hydrolase
	SMART	SM00487	ultrahead3	225	436	5.50E-64	IPR014001	Helicase superfamily 1/2, ATP-binding domain
	MobiDBLite	mobidb-lite	consensus disorder prediction	602	628	-	-	-
	CDD	cd18052	DEADc_DDX4	164	427	0	-	-
	MobiDBLite	mobidb-lite	consensus disorder prediction	11	26	-	-	-
	SUPERFAMILY	SFS2540	P-loop containing nucleoside triphosphate hydrolases	284	565	4.61E-73	IPR027417	P-loop containing nucleoside triphosphate hydrolase
XP_008415818.1 piwi-like protein 2 [Poecilia reticulata]	Gene3D	G3DSA:2.170.260.10	paz domain	468	592	1.10E-38	-	-
	MobiDBLite	mobidb-lite	consensus disorder prediction	113	145	-	-	-
	Pfam	PF02170	PAZ domain	473	605	4.60E-32	IPR003100	PAZ domain
	PANTHER	PTHR22891:SF111	PIWI-LIKE PROTEIN 2	189	1055	0	-	-
	SMART	SM00950	Piwi_a_2	750	1041	9.00E-123	IPR003165	Piwi domain
	MobiDBLite	mobidb-lite	consensus disorder prediction	239	263	-	-	-
	CDD	cd02845	PAZ_piwi_like	468	586	9.18E-55	-	-
	CDD	cd04658	Piwi_piwi-like_Euk	594	1038	0	-	-
	SUPERFAMILY	SSF101690	PAZ domain	316	625	1.29E-71	IPR036085	PAZ domain superfamily
	ProSiteProfiles	PSS0821	PAZ domain profile.	469	584	21.01985	IPR003100	PAZ domain
	Gene3D	G3DSA:3.40.50.2300	-	677	806	2.40E-31	-	-
	PANTHER	PTHR22891	EUKARYOTIC TRANSLATION INITIATION FACTOR 2C	189	1055	0	-	-
	SMART	SM00949	PAZ_2_a_3	469	608	2.40E-61	IPR003100	PAZ domain
	Gene3D	G3DSA:3.30.420.10	-	815	1051	1.50E-74	IPR036397	Ribonuclease H superfamily
	ProSiteProfiles	PSS0822	Piwi domain profile.	750	1041	43.52801	IPR003165	Piwi domain
	Pfam	PF02171	Piwi domain	750	1040	9.20E-82	IPR003165	Piwi domain
	SUPERFAMILY	SSF53098	Ribonuclease H-like	602	1055	9.36E-130	IPR012337	Ribonuclease H-like superfamily
	CDD	cd00105	KH-I	154	219	7.16E-14	-	-
XP_008436386.1 tudor and KH domain-containing protein isoform X1 [Poecilia reticulata]	Phobius	TRANSMEMBRANE	Region of a membrane-bound protein predicted to be embedded in the membrane.	44	62	-	-	-
	Pfam	PF00013	KH domain	155	220	6.50E-14	IPR004088	K Homology domain, type 1
	Gene3D	G3DSA:3.30.310.210	-	100	227	2.80E-16	-	-
	Gene3D	G3DSA:2.30.30.140	-	363	435	1.20E-66	-	-
	SUPERFAMILY	SSF54791	Eukaryotic type KH-domain (KH-domain type I)	151	224	2.92E-15	IPR036612	K Homology domain, type 1 superfamily
	SMART	SM00322	kh_6	151	223	1.10E-13	IPR004087	K Homology domain
	Phobius	NON_CYTOPLASMIC	Region of a membrane-bound protein predicted to be outside the membrane, in the extracellular region.	63	578	-	-	-
	PANTHER	PTHR22948:SF18	TUDOR AND KH DOMAIN-CONTAINING PROTEIN	43	566	1.10E-114	-	-
	Pfam	PF00567	Tudor domain	328	450	6.90E-25	IPR002999	Tudor domain
	Phobius	TRANSMEMBRANE	Region of a membrane-bound protein predicted to be embedded in the membrane.	12	32	-	-	-
	Phobius	CYTOPLASMIC_DOMA	Region of a membrane-bound protein predicted to be outside the membrane, in the cytoplasm.	33	43	-	-	-
	ProSiteProfiles	PSS0304	Tudor domain profile.	380	439	10.28092	IPR002999	Tudor domain
	PANTHER	PTHR22948	TUDOR DOMAIN CONTAINING PROTEIN	43	566	1.10E-114	-	-
	SUPERFAMILY	SSF63748	Tudor/PWWP/MBT	356	451	5.19E-22	-	-
	ProSiteProfiles	PSS0084	Type-1 KH domain profile.	152	218	16.14333	-	-
	Gene3D	G3DSA:2.40.50.90	-	334	519	1.20E-66	IPR035437	SNase-like, OB-fold superfamily
	SMART	SM00333	TUDOR_7	379	437	1.10E-04	IPR002999	Tudor domain
	CDD	cd04508	TUDOR	384	431	2.48E-11	IPR002999	Tudor domain
	Phobius	NON_CYTOPLASMIC	Region of a membrane-bound protein predicted to be outside the membrane, in the extracellular region.	1	11	-	-	-
XP_008436387.1 tudor and KH domain-containing protein isoform X2 [Poecilia reticulata]	Pfam	PF00567	Tudor domain	296	418	6.30E-25	IPR002999	Tudor domain
	TMHMM	TMhelix	Region of a membrane-bound protein predicted to be embedded in the membrane.	13	30	-	-	-
	Gene3D	G3DSA:3.30.310.210	-	68	195	2.50E-16	-	-
	PANTHER	PTHR22948:SF18	TUDOR AND KH DOMAIN-CONTAINING PROTEIN	11	534	1.00E-114	-	-
	SUPERFAMILY	SSF63748	Tudor/PWWP/MBT	324	419	4.74E-22	-	-
	Phobius	TRANSMEMBRANE	Region of a membrane-bound protein predicted to be embedded in the membrane.	12	30	-	-	-
	Gene3D	G3DSA:2.30.30.140	-	331	403	1.00E-66	-	-
	Phobius	NON_CYTOPLASMIC	Region of a membrane-bound protein predicted to be outside the membrane, in the extracellular region.	31	546	-	-	-
	SUPERFAMILY	SSF54791	Eukaryotic type KH-domain (KH-domain type I)	119	192	2.78E-15	IPR036612	K Homology domain, type 1 superfamily
	Pfam	PF00013	KH domain	123	188	6.00E-14	IPR004088	K Homology domain, type 1
	Phobius	CYTOPLASMIC_DOMA	Region of a membrane-bound protein predicted to be outside the membrane, in the cytoplasm.	1	11	-	-	-
	ProSiteProfiles	PSS0084	Type-1 KH domain profile.	120	186	16.14333	-	-
	ProSiteProfiles	PSS0304	Tudor domain profile.	348	407	10.28092	IPR002999	Tudor domain
	SMART	SM00333	TUDOR_7	347	405	1.10E-04	IPR002999	Tudor domain
	PANTHER	PTHR22948	TUDOR DOMAIN CONTAINING PROTEIN	11	534	1.00E-114	-	-
	Gene3D	G3DSA:2.40.50.90	-	302	487	1.00E-66	IPR035437	SNase-like, OB-fold superfamily
	CDD	cd04508	TUDOR	352	399	1.82E-11	IPR002999	Tudor domain
	CDD	cd00105	KH-I	122	187	7.38E-14	-	-
	SMART	SM00322	kh_6	119	191	1.10E-13	IPR004087	K Homology domain

Functional domains predicted with InterProScan in *Poecilia reticulata* proteins Vasa (XP_008428196.1), PIWI (XP_008415818.1), TDRKH isoform X1 (XP_008436386.1) and TDRKH isoform X2 (XP_008436387.1). Highlighted rows indicate predicted domain (with e-value < 0.05) included in the antibody binding regions.

The multiple sequence alignment result as produced by T-coffee.

Cedric Notredame

SCORE=936

BAD AVG GOOD

GeneTex : 92

XP 008436386.1 : 91

coñs : 93

GeneTex **MSTER**-----**TSWT**-----**SLSTIQKIALGLGIPASATVAYILYRRYR**
 XP_008436386.1 **MDVGVS**KSRVFSYSSQ**VLLSKCS**IPLSVRY**VM**DAVKD**GPRGKM**VALAAGLSVGATIGYIVYRHIS

cons * * ** * ** . ** . ** .

GeneTex ESREERLTFVGEDDIEIEMRVPQEAVKLIIGROGANIKQLRKQTGARIDV--DTEDVGDERVL--L
XP_008436386.1 NASSSQEP----DTEESKIILPIEVYRNISRCYATFLDVASQKSGAHVRVASYSEETGHKAAVCVO

cons

GeneTex
XP_008436386.1

cons * * ** * * . * * * **** ** .***** . . * . . .***** * . . .

GeneTex TLLLSRLIKISGTOKEVAAAKHLILEKVSEDEELRKRIAHSAETRVPRKQIPISVRREDMTEPGGAG
XP_008436386.1 NPGGKGSVTITGSKOEVKOAKEMILERVGADAVVRKISOSSALROKRGHKVV-----

cons . . . * . * . * . * . * . * . * . * . * . * . *

GeneTex
XP_008436386.1

cons

GeneTex
XP_008436386.1

cons . . . * . . . ***** . . . * . . . ***** . . . ***** . . . * . . . ***** . . . * . . . * . . . *

GeneTex DL---TVHVGDI VAAPLPTNGSWYRARVLGTL^{EN}GNLDLYFVDFGNGDCPLKDLRA-----
XP_008436386.1 EQRMSILVGDIVAAPYRDYKNWRARVLGFLRSGLV^{LD}LYYVDFGNGEFSRDLRPLRSDFLSLP

cons . . . ***** * ***** * * .*****.*****. **

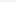

GeneTex
XP_008436386.1 FOAIECSLAGVRPKGEAWTEAALDIFEQLTYCANWRPLOAKLCSYSHSEVSSWSPVKLYDNSKGKA

cons

GeneTex
XP_008436386.1

cons

GeneTex -----L
XP_008436386.1 VEDELL

cons   *

T-Coffee alignment of TDRKH isoform X1 of *P. reticulata* (XP_008436386.1; 579 amino acids) and TDRKH GeneTex antibody binding site (406 amino acids).

The multiple sequence alignment result as produced by T-coffee.

```
*
XP_008428196.1      : 94
tr|042107|04210      : 91
cons                 : 96
```

XP_008428196.1 GKK-----GRGRGGFWNSSADGDSRSDNEDGERHGF
tr|Q42107|Q4210 GGRGGSRRGGRGGFSGFKSEIDENGSDGGWNGGESRGRGRGGFRGGFRSGSRDENDENRNDDGW

cons ** : * * * * *

XP_008428196.1
tr|042107|04210

SGRVGRGRGRG-FNRMNSDGFSED-----GDGAHENG-FRGRGRGGRRGGGFRQ
KGGESRGRGRGGFGGSFRGGFRDGGNEDTGRRGFGRENNENGNDGEGSEGRGRGRGGFRGGFRD

cons

* ***** * ** : * * * * * * * * * *

XP_008428196.1
tr|Q42107|Q4210

DA--EQGGRRGFRGGYRGKDEEAFSPGEDQGPVKD-DPDSDKPRVTVPPPTLPEDEDSIFSHY
GGGDESCKRGRFGRGGFRGRNEEVFSKVTTADKLQEGSENAAGPKVVVYPPPPPEEESSIFSHY

cons

. . * * ** *** : * : * * * * . . . : . . . : * : * . **** * : * . *****

```
XP 008428196.1      KSGINFDKYDDILVDISGTPPPRAIITFDEAALCESLRKNISKSGYVKPTPVQKHGIPIISAG
tr|042107|04210     ATGINFDKYDDILVDVSGNSPPKAIMTFEEAGLCDSLSKNVSKSGYVKPTPVQKHGIPIISAG

cons                : **** *: * ** : * : * : * : * : * : * : *
```

```
XP_008428196.1      RDLMACAQTGSGKTA AFLLPILQLMTDGVAA SRFSETQEPEAVIVAPTRELINQIYLEARKF
tr|042107|04210     RDLMACAQTGSGKTA AFLLPILQRFMTDGVAA SKFSEIQEPEAII VAPTRELINQIYLEARKF

cons                *****.*****.*** *****.*****
```

```
XP_008428196.1      AHGTCVRPVVYGGVSTGYQIREILKGCNVVCGTGRLLDMIGRGKVLGSKVRYLVLDEADM
tr|042107|04210     AYGTCVRPVVYGGINTGYTIREVLKGCNVLCATPGRLLHDLIGRGKIGLSKVRYLVLDEADM

cons                *.*****.*** ***.*****.*.*****.*.*****.*****.*****
```

```

XP_008428196.1      LDMGFEPDMRRLVGSPGMPSENKRNQTLMFSAATYPEDIQMAADFLKPDYFLAVGVGGACSD
tr|042107|04210     LDMGFEPDMRRLVGSPGMPSEERQTLMFSAATYPEDIQMAADFLKVDYIFLAVGVGGACSD
cons                *****.*.*.******.*****.*****.*****.*****.*****

```

```
XP_008428196.1      VEQKFVQVTKFSKREQLLDILKTGTERTMVFVETKRQADFIAVFLCQEKVPTTSIHGDREQR  
tr|042107|04210     VEQTVVQVDQYSKRDLLELLRATGNERTMVFVETKRSADFIATFLCQEKISTTSHGDREQR  
  
cons               ***   **       :***.***.*..** *****          ****          .*****
```

```

XP_008428196.1      ERELALTDFRSGKCPVLVATSVAAAGLDIPDVQHVHVNFDLPKDIDEYVHRIGRTGRCGNVGRA
tr|042107|04210     EREKALSDFRLGHCPLVATSVAAAGLDIEQVQHVVNFDMPSSIDEYVHRIGRTGRCGNTGRA
cons                ***  *.*.*.*  *.*****.*****.*.*****.***

```

```
XP_008428196.1      VSFFDPEADGGLARSLVTVLSKAQQEVPPWLEESAFSSHG-AGFNPK-KTFGSTDSRKTSFQ
tr|042107|04210     VSFNPESDTPLARSLVKVLSGAQQVVPKWLEEVAFAHGTGTFNPRGVFASTDSRKGGSFK

cons                ****.*.* ***** ** * * * * *.** :****. *.****** *
```

XP_008428196.1
tr|042107|04210
cons

T-Coffee alignment of Vasa from *P. reticulata* (XP_008428196.1; 640 amino acids) and *Danio rerio* (tr|O42107|O42107 DANRE; 716 amino acids). Red box indicates anti-VASA binding site.

The multiple sequence alignment result as produced by T-coffee.

BAD AVG GOOD

```

XP_008415818.1  MDPKPKPPD-----LSDNAGFQMLGR-GRGLQPVEMAVGRSRLGLLSAEGGLGLGRAGFLPPGDI
NP_060538.2     MDPFRPSPFRGQSPIHPSQCQAVRMPGCVQASKPLDPALGRG-----A

```

cons *** : * . * : . . : * * : . : * : : * : * * .

XP_008415818.1 PAGRGVLPSSSTAPGRGLLVQPDEVGVGRRARGLLLPSAEPRVGVSRGAVLPRLEQQHEQKHMLETTP
NP_060528.2 D AGRGIVVECKRFEEDSTDP

cons *

XP_008415818.1 ASAGDPAAPRGEEVSAPPCGQGSTLVSMFRGMGVTWGR-----GTP-----AVGRGESGD-----

cons

XP_008415818.1 -----GGEVKVQGSLSVGLTTAMQAGAGHRGDSMGRGSSLCQPMVVGLGRAALP-QLG
NP_060538.2 REELSPTFWDPKVLAAAGDSKMAETSVGWS-----RTLGRGSSDAS--LLPLGRAAGGISRE

cons

XP_008415818.1 VGRGQALLSALPSGQIKPVSPSTDPQTAPLSPPHPEGVLKVVPMTQDLPVPLSSAQPCKEMTMEAV
NP_060538.2 VDKPCTFTSPSRGPPQLSSPPALPQ-----SPLHSPDRPLVLTVEHKEKEL-----

cons * . : . : * : . * : ** . : ** : * * : * : : : ** :

XP_008415818.1 HTPINKTGKGAPITIGSNHIVVSCKNEAVYQYHVTFTPNVESMAMRFGMMDHRSTTGEVVAFDG
NP_060538.2 ---IVKQSGKGPQSLGLNLVKIQCHNEAVYQYHVTFSNVECKSMRFGMLKDHAQVGTGNVTAFDG

cons

XP_008415818.1 SILYLPVKLKDEVLLKSSRRTDNQEIEIKIQMTKILPNCDCIPFYNVVFRVRMVKIIGLKQVARN
NP_060538.2 SILYLPVKLKQVLELKSQRKTDSEISIKIQMTKILEPCSDLCIPFYNVVFRVRMVKLLDMKLVGRN

```
cons *****: : : ***. *.** . ** .***** * ,*****: : : * *,**
```

XP_008415818.1 HYDPESAVVLEKQRLQVWPGYATAIKRTDGGLYLSVEVTHKVLQNSVLDLNMMLYRQSKENFQDV
NP_060538.2 FYDPTSAMVLQQHRLQIWPGYASIRRTDGGFLFADVSHKVIKRDVLDVMHAIYQQNKHFQDE

cons . *** ** : ** : : ** : ***** : : * : ***** : * : : * : ***** : ** : ***** : * : : * : * : ** : *****

XP_008415818.1 CTKELVGAIVITRYNNRTYRIDSI EWNKSPNDTFTLMDGKTTFLEYYSKNYGITIKEMNQPLLH
NP_060538.2 CTKLLVGNIVITRYNNRTYRIDDVDWNKTPKDSFTMSDGKEITFLEYYSKNYGITVKEEDQPLLH

cons

XP_008415818.1 RPKERSRPGGKQIITGEILLVPELSFLTGIPEKMRKMDRAMKELTNHINVSSSEQHTNSIKQLLKNI
NP_060538.2 RPSEQRQDNHG-MLLKGEILLPELSFMTGIPEKMKKDFRAMKDLAQQINLSPKQHHSALECLLQRI

cons **,**,* * :,: *****:*****:*****:**:*:**:*:*:*:*:*:*:*:*:

XP_008415818.1 SSNPESVKELSRWGLEIGSEILIVQGRTPLETICLQTSLIPTGADVSWSEVVVDTSISSVPLNI
NP_060538.2 AKNEAATNELMRWGLRLQDKVHKIEGRVLPMERINLKNTSFITSQELNWKVEVTRDPSLTIPMHF

cons : * : : ** **** : : : : : : ** : ** : * * * : : : : : * , : : : * : ** : ** : ** : : * : :

XP_008415818.1 WAIFYPSRCADQAEELVSTFKKVAGPIGVRMARPIRVELRDDRTETVKSIIHSLTSEPNLQLVVC
NP_060538.2 WALFYPKRAMDQARELVNMLEKTAGPTIGMRMSPPAWVELKDDRTETVYRTIOSTLGAEGKTOMVVC

cons **;***.*.***.***.;;*:*****;*: * ***;*** *****;*:;* *;*;*;*:***

XP_008415818.1 IMVGNRDDLYSAIKKLCCVKSPISQAINIRTISQMKLKSVAQKILLQVNSKLGGLWTVNIPLK
NP_060538.2 IIMGPRDDLYGAIKKLCCVQSPVPSOVVNVRTIGOPTRLRSVAQKILLQINCKLGGELWGVDIPLK

cons *:;* *****.*****:***:***:;*:***:* *:;*****:;* ***** *:*****

XP_008415818.1 NLMVGVGDVHHDTSKSHQSVMGFVASVNSSLTRWYSRVTFQTPSEELIHGFRVCLLAAALQKYHEIM
NP_060538.2 QI MVTGMDDVYHDPSSRGMRSSVGFVASTNI TI TKWYSRVVFOMPHQETVDSI K I C I VGS I KKEYEVM

cons .***.*.**.*.*.*.***.*****.***.******.**.*.*..**.*.*.*.*.

XP_008415818.1 HNLPEKIVVYRDGVSVDGOLKMQVEQYEIPQLIKCFETFPSYEPKLVFIVVQKRISTNLYAWASNSFG
NP_060538.2 HCLPEKTVVYRDGVSVDGOLKTVANYETPOLQKCEFAFENYOPKMQVEVVOVKKTSTNIYI AAPQNEV

cons * **** * : **** * : * : * : * : **** : **** * : *

XP_008415818.1 TTPPGTVLDHTLTQKDWDFYFLMAHHIRQGCGLPHTHYISLYNTANLSPDHLQRLTFKMCHLYWNWP
NP_060538.2 TTPPGTVVDHTITSCFWDVEYI IAHVVRGCGTPTHYVCVI NTANI SPDHMORI TEKI CHMYWNWP

```
cons      **  ****.***.*      .*****.***.*****.*****.      .      .*****.*****.***.*****
```

XP_008415818.1 GTIRVPAPCKYAHKLAFLSGQYLHSEPAIQLSDKFLFL
NP_060538.2 GTIRVPAPCKYAHKLAFLSGHTLHHEPATOLCENLFFL

cons ***** . ** ***** . *****

T-Coffee alignment of PIWI from *P. reticulata* (XP_008415818.1; 1056 amino acids) and *Homo sapiens* (NP_060538.2; 974 amino acids). Red box indicates anti-PIWI binding site.

The multiple sequence alignment result as produced by T-coffee.

*

*

cons : 94

cons

cons

cons * * ** * * : * * * * * * *

cons . : *:*:** **:*:*:*:* *

cons

```
cons      : . . . * . ***** . ** . ** . ***** . ***** . * ***** . ** . * * *
```

cons : ***** * ***** * * ***** ***** ** *

cons ***** : *.*: * * **** *.**:**.**:**.*** **.*** :. :*.**.* : ****.***

cons :*** **::*:*:*: *::*::::***:*****

cons ***: ** ** : ** : **

T-Coffee alignment of TDRKH from *P. reticulata* (XP_008436386.1; 579 amino acids) and *Homo sapiens* (NP_001077432.1; 562 amino acids). Red box indicates anti-TDRKH binding sites.